Persistent currents from Berry's phase in mesoscopic systems

Daniel Loss* and Paul M. Goldbart†
Department of Physics, University of Illinois at Urbana-Champaign, 1110 West Green Street, Urbana, Illinois 61801-3080 and Beckman Research Institute, University of Illinois at Urbana-Champaign, 1110 West Green Street, Urbana, Illinois 61801-3080
(Received 1 July 1991; revised manuscript received 20 February 1992)

The quantum orbital motion of electrons in mesoscopic normal-metal rings threaded by a magnetic flux produces striking interference phenomena such as persistent currents due to the Aharonov-Bohm effect. Similarly, when a quantum spin adiabatically follows a magnetic field that rotates slowly in time, the phase of its state vector acquires an additional contribution known as the Berry phase. We explore the combination of these two quantum phenomena by examining the interplay between orbital and spin degrees of freedom for a charged spin-$\frac{1}{2}$ particle moving in a mesoscopic ring embedded in a classical, static inhomogeneous magnetic field, i.e., a texture. As a consequence of its orbital motion through the texture, the spin experiences, via the Zeeman interaction, a varying magnetic field. This results in a Berry — or geometric — phase, leading to persistent (i.e., equilibrium) currents of charge and spin. These mesoscopic phenomena are related to (but should be distinguished from) the conventional persistent currents that result from magnetic flux *through* a ring. We develop a path-integral approach to decouple the orbital and spin motion and, by using an adiabatic approximation, we compute the equilibrium expectation values of the persistent charge and spin currents and the magnetization. We find that the persistent currents depend on the texture in a striking manner through a geometric phase (related to a surface area characterizing the texture) and a geometric vector (related to the projections of this area). In the special case of a cylindrically symmetric texture we use a spectrum obtained by Kuratsuji and Iida to obtain exact results that confirm, independently, the validity of the path-integral approach in the adiabatic limit. We discuss the connection between the geometric vector and quantum-mechanical correlations, and examine quantum fluctuations and the zero-point energy.

I. INTRODUCTION AND OVERVIEW

The electromagnetic vector potential, as shown by Aharonov and Bohm,[1] influences the quantum-mechanical orbital motion of electrons, and other charged particles, even if the particles move solely through regions of vanishing electric and magnetic fields. This purely quantum-mechanical effect manifests itself through the acquisition of a *phase factor* which can change the boundary condition on the orbital wave function. If the orbital motion of the electron is confined to a multiply connected region, such as a ring, then this Aharonov-Bohm phase factor can cause striking quantum interference phenomena. In quantum transport, for example, the magnetoconductance of disordered doubly connected metal samples oscillates as a function of the enclosed magnetic flux.[2]

Equally striking interference phenomena occur in thermal equilibrium. In particular, as pointed out by Büttiker, Imry, and Landauer,[3,4] a normal-metal ring in equilibrium threaded by a magnetic flux will exhibit a *persistent* charge current which oscillates with the flux. Observation of this effect in a sample consisting of approximately 10^7 disconnected Cu loops has recently been reported by Lévy *et al.*[5] Even more recently, Chandrasekhar *et al.*[6] have reported observing the persistent current in a *single* Au loop. Phenomena such as these are restricted to mesoscopic systems, by which we mean systems whose size is sufficiently small that the orbital motion remains quantum phase coherent throughout. Furthermore, it should be emphasized that the persistent currents considered here occur in the *normal* state and are not a manifestation of superconductivity.

Recognizing the significance of the Aharonov-Bohm phase factor in conventional persistent currents, we are motivated, then, to identify an alternative source of quantum-mechanical phase factor which can produce analogous equilibrium currents. Now, as observed by Berry,[7,8] when a quantum-mechanical spin adiabatically follows a magnetic field which rotates slowly in time, the phase of its wave function acquires an additional contribution known as the Berry — or geometric — phase. To exploit this geometric phase in the context of mesoscopic

physics, and thus produce persistent currents, we shall analyze the equilibrium state of a system consisting of spin-$\frac{1}{2}$ particles confined to a mesoscopic ring which we suppose to be embedded in a *static* inhomogeneous magnetic field, i.e., a texture such as that depicted in Fig. 1. Due to their Zeeman interaction with this texture the particles, as they orbit the ring, are subject to a varying magnetic field. In the adiabatic limit a geometric phase then arises, causing persistent currents, but now of both charge and spin, through a mechanism closely related to that causing conventional persistent currents.

The Aharonov-Bohm phase emerges *exactly* from the form of the coupling between the particle and the electromagnetic vector potential. In contrast, the geometric phase arises in an approximation — the adiabatic approximation — and is not of such general validity. Nevertheless, this adiabatic approximation is applicable to a broad range of experimentally accessible systems.[9] In the present paper we develop a detailed description of the equilibrium state for spin-$\frac{1}{2}$ particles moving through an *arbitrary* texture, and obtain explicit expressions for the resulting persistent charge and spin currents and magnetization. Results for the special case of symmetric textures have been reported in an earlier paper.[10]

We approach the issue of persistent currents caused by arbitrary textures by constructing a tractable Feynman-path-integral representation for the thermal propagator. This representation has the virtue of allowing us to implement the adiabatic approximation in a form related to that analyzed by Berry,[7] and thus to identify the analog of the Aharonov-Bohm phase responsible for equilibrium currents. This type of approach is quite general and will, we hope, find application in a broad class of problems, both in thermal equilibrium and in transport.

The primary reason for developing this path-integral method is that the direct approach via the solution of the time-independent Schrödinger equation in the presence of an arbitrary texture is generally intractable. Such an approach is only possible for the very special case of a cylindrically symmetric texture, for which we also present the direct approach below. Results from this symmetric texture provide independent confirmation of the validity of the path-integral approach.

We shall find that the path-integral approach, together with the adiabatic approximation, leads to results for the persistent currents with a strikingly geometrical character. These currents are found to depend on the texture through the geometric phase, which is related to the surface area on the unit sphere (in the space of magnetic fields) enclosed by the texture. In addition, the spin current is found to depend on some geometric information, the components of a geometric vector, which are related to the *projection* of this surface area on to the associated equatorial planes.

This paper is organized as follows. In Sec. II we present an idealized model of a strictly one-dimensional system consisting of noninteracting spin-$\frac{1}{2}$ particles coupled to an inhomogeneous texture via a Zeeman term. In Sec. III we introduce the physical quantities upon which we shall focus our attention, namely the charge current, the spin current, and the magnetization. In Sec. IV we develop the path integral for arbitrary textures by constructing the thermal propagator. This will lead us to a form of the path integral in which spin and orbital motion are, in a sense to be made precise below, decoupled, thus allowing us to invoke the adiabatic approximation, following Berry, for the (imaginary-time) spin dynamics. Then, by explicitly decompactifying the orbital path integral, we introduce a convenient winding number representation. In Sec. V we give detailed results for observable quantities for textures with constant magnitude but which are otherwise arbitrary. Here, we also discuss the geometric vector and its relation to quantum-mechanical correlations, and give a heuristic picture of the origin of the persistent currents. In addition, we give the results of the adiabatic approximation to the path integral specialized to the case of the symmetric texture. In Sec. VI we describe the exact solution for the case of symmetric textures by finding the spectrum of energy eigenvalues and using them to compute physical quantities. We also give explicit results for the case of the planar texture and, furthermore, discuss the limit in which the exact diagonalization and path-integral approaches are equivalent. In addition, quantum fluctuations and zero-point energy are discussed here. In Sec. VII we give the results for equilibrium currents and magnetization for a system of many noninteracting spin-$\frac{1}{2}$ fermions. We conclude, in Sec. VIII, with a summary of our results, and mention some interesting future directions.

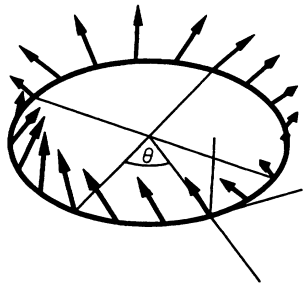

FIG. 1. Mesoscopic ring (thick circle) in an inhomogeneous magnetic field (arrows) with tilt angle $\chi(\theta)$ and twist angle $\eta(\theta)$.

II. THE MODEL

We begin by considering a single particle of mass m, charge q, spin-$\frac{1}{2}$, and gyromagnetic ratio g, confined to a ring of radius a. The ring is embedded in a specified static inhomogeneous magnetic field $\mathbf{B}(\theta)$, as depicted in Fig. 1, and is taken to be strictly one dimensional. We shall neglect particle-particle interactions. The position of the particle is specified by the angular coordinate θ, and the Hamiltonian for this system is then taken to be

$$\hat{H} = \hat{H}^{\text{orb}} - g\mu\mathbf{B}(\hat{\theta})\cdot\hat{\boldsymbol{\sigma}}, \tag{2.1}$$

$$\hat{H}^{\text{orb}} = \frac{1}{2ma^2}\left(\hat{p}_\theta - qa\hat{A}_\theta\right)^2 + V(\hat{\theta}),$$

where $\hat{p}_\theta$ is the angular momentum operator conjugate to the coordinate operator $\hat{\theta}$, $\hbar\hat{\sigma}^k/2$ (with $k = 1,2,3$) are the Cartesian components of the spin operator $\hat{\mathbf{S}}$, $2\mu = |q|\hbar/2m$ (i.e., the Bohr magneton if the particle is an electron), and V is an arbitrary potential periodic in θ. We assume that the particle is physically confined to the one-dimensional ring by an external potential; thus the kinematic velocity operator transverse to the ring $\hat{\mathbf{v}}_\perp = (\hat{\mathbf{p}} - q\hat{\mathbf{A}})_\perp/m$ vanishes.

We shall refer to the static classical inhomogeneous magnetic field $\mathbf{B} = \nabla \times \mathbf{A}$ as a *texture*. This texture can have an *arbitrary* configuration, provided that its spatial variation is not rapid enough to invalidate the adiabatic approximation that we shall describe below. The device causing the texture on the ring will typically also cause a magnetic flux through the ring, which is accounted for by the minimal coupling to the vector potential $\mathbf{A}$. One might attempt to produce a texture by, e.g., locating the mesoscopic ring between a pair of mesoscopic Helmholtz coils, with the current in one coil reversed. Alternatively, the ring could be fabricated from an intrinsically ferromagnetic material, or supported on an inhomogeneous, insulating ferromagnetic substrate.

We emphasize that for inhomogeneous textures the Zeeman term $g\mu\mathbf{B}(\hat{\theta})\cdot\hat{\boldsymbol{\sigma}}$ couples the spin and orbital degrees of freedom. Besides electrons, such a coupling can also be experienced by neutral particles with spin, e.g., neutrons and ^{3}He atoms. We have, for the sake of simplicity, omitted from the Hamiltonian any conventional spin-orbit coupling caused, e.g., by the potential which confines the electron to the ring.[11] The Zeeman interaction causes an *effective spin-orbit* coupling which should be distinguished from the consequences of conventional spin-orbit coupling.[12]

III. OBSERVABLE QUANTITIES

We shall focus our attention on three physical equilibrium quantities, the magnetization vector $\hbar\langle\hat{\sigma}^k\rangle/2$, the charge current $(q\hbar/2\pi ma^2)\langle\hat{J}^0\rangle$, and the spin current vector $(\hbar^2/4\pi ma^2)\langle\hat{J}^k\rangle$, where $k = 1,2,3$ labels Cartesian components. The dimensionless current operators[13] $\hat{J}^\mu$ are given by

$$\hat{J}^\mu = \frac{1}{\hbar}\left(\hat{p}_\theta - qa\hat{A}_\theta\right)\hat{\sigma}^\mu , \tag{3.1}$$

where $\mu = 0,1,2,3$, and where, for the sake of convenience, we have introduced the identity operator $\hat{\sigma}^0 = \hat{\mathbb{1}}$. For neutral particles $q = 0$, and it is of course the mass current $(1/2\pi a^2)\langle\hat{p}_\theta\rangle$ rather than the charge current which is of interest. The brackets $\langle\cdot\rangle$ denote equilibrium expectation values computed in the canonical ensemble, i.e., $\langle\cdot\rangle = Z^{-1}\,\mathrm{Tr}\,(\cdot)\exp\left(-\beta\hat{H}\right)$, where $\beta = 1/k_BT$ measures the inverse temperature T, the canonical partition function is denoted by Z, and Tr denotes a trace taken over single-particle states. Below, when discussing the consequences of Fermi-Dirac statistics for many-particle systems, we shall also mention the grand canonical ensemble.

The reason for focusing on the currents defined above is that they exhibit the following essential fact: for a generic texture the *equilibrium* state is a current-carrying state. The currents are a manifestation of *quantum-mechanical interference* which is geometrically induced by the texture. We emphasize that these currents are equilibrium currents and therefore persist indefinitely and cannot be dissipated. These are *not* nonequilibrium currents of the type driven by an external force, and they do not possess a classical analog. As we shall see, these persistent currents vanish in the classical limit, the high-temperature limit, and the macroscopic (i.e., thermodynamic) limit. Thus, they represent truly mesoscopic quantum-mechanical effects.[14]

The currents described here bear some similarities with the charge current caused by Aharonov-Bohm interference,[1] e.g., in mesoscopic metal rings threaded by magnetic flux.[3,4] These similarities can be seen most clearly within a version of the adiabatic approximation, given below, in which the geometric phase[7] plays a role analogous to the Aharonov-Bohm phase. In addition, we shall find that the spin current is partly characterized by a *geometric vector*, which encodes geometric information about the texture distinct from that contained in the geometric phase. Finally, it should be emphasized that, in contrast with conventional persistent currents, the currents caused by the texture can occur in neutral systems with spin, such as normal ^{3}He.

IV. PATH INTEGRAL FOR ARBITRARY TEXTURES

We now construct a path-integral representation of the thermal propagator describing the statistical mechanics of a quantum-mechanical spin-$\frac{1}{2}$ particle confined to a ring in the presence of an arbitrary magnetic texture. This propagator, evaluated within an adiabatic approximation which illuminates the role of the geometric phase, will be used to compute the partition function, the equilibrium expectation values of the charge and spin currents, and the magnetization, introduced in Sec. III.

A. Expectation values and thermal propagator

We consider a particle governed by the Hamiltonian $\hat{H}$, Eq. (2.1), and introduce the following convenient complete set of states:

$$|\theta;\alpha\rangle = |\theta\rangle \otimes |\alpha\rangle, \tag{4.1}$$

with $0 \le \theta < 2\pi$ and $\alpha = \pm 1$. These states are simultaneous eigenstates of $f(\hat{\theta})$ (where f is periodic) and, say, $\hat{\sigma}^3$, i.e., $f(\hat{\theta})\,|\theta\rangle = f(\theta)|\theta\rangle$ and $\hat{\sigma}^3\,|\alpha\rangle = \alpha|\alpha\rangle$. (Later, in the calculation of the spin current and the magnetization, it will be convenient to replace $|\alpha\rangle$ by a basis in which either $\hat{\sigma}^1$ or $\hat{\sigma}^2$ is diagonal.) Furthermore, we impose the physical choice that all states are periodic functions of θ. This choice is obtained through the requirement that the

orbital state $|\theta\rangle$ is a periodic function of θ. Of course, all operators must be periodic, i.e., they must not take states out of the physical space of states obeying periodic boundary conditions.

To obtain the equilibrium expectation value $\langle\hat{\mathcal{O}}\rangle$ of some observable $\hat{\mathcal{O}}$ we calculate the thermal propagator

$$G(\theta_f,\alpha_f;\theta_i,\alpha_i)=\langle\theta_f;\alpha_f|e^{-\beta\hat{H}}|\theta_i;\alpha_i\rangle \tag{4.2}$$

in terms of which $\langle\hat{\mathcal{O}}\rangle$ becomes

$$\langle\hat{\mathcal{O}}\rangle=\frac{1}{Z}\sum_{\alpha_i,\alpha_f=\pm1}\int_0^{2\pi}d\theta_i\int_0^{2\pi}d\theta_f\,\langle\theta_i;\alpha_i|\hat{\mathcal{O}}|\theta_f;\alpha_f\rangle \times G(\theta_f,\alpha_f;\theta_i,\alpha_i)\,. \tag{4.3}$$

B. Decoupling of spin and orbital motion

We calculate $G(\theta_f,\alpha_f;\theta_i,\alpha_i)$ by constructing a path-integral representation for it. In the integrand of this representation the orbital and spin degrees of freedom factorize, in the sense that the spin evolves (in imaginary time) in the presence of an external magnetic field which depends parametrically on the Feynman path of the orbital motion.[15] This representation is achieved through a straightforward extension of the standard technique[16,17] of inserting the resolution of the identity,

$$\hat{\mathbb{1}}=\sum_{\alpha=\pm1}\int_0^{2\pi}d\theta\,|\theta;\alpha\rangle\,\langle\theta;\alpha|, \tag{4.4}$$

at infinitesimally separated imaginary-time slices $\tau_j = j\beta/N = j\epsilon$ (with $j=1,2,\ldots,N-1$) which leads to the representation

$$\begin{aligned}G(\theta_f,\alpha_f;\theta_i,\alpha_i)&=\langle\theta_f;\alpha_f|\,e^{-\epsilon\hat{H}}\cdots e^{-\epsilon\hat{H}}\,|\theta_i;\alpha_i\rangle\\&=\sum_{\alpha_1\ldots\alpha_{N-1}}\int_0^{2\pi}d\theta_1\cdots d\theta_{N-1}\,\langle\theta_f;\alpha_f|e^{-\epsilon\hat{H}}|\theta_{N-1};\alpha_{N-1}\rangle\cdots\\&\quad\times\langle\theta_j;\alpha_j|e^{-\epsilon\hat{H}}|\theta_{j-1};\alpha_{j-1}\rangle\cdots\langle\theta_1;\alpha_1|e^{-\epsilon\hat{H}}|\theta_i;\alpha_i\rangle\,.\end{aligned} \tag{4.5}$$

The matrix elements are then evaluated using the Baker-Campbell-Hausdorff formula $\exp(-\epsilon\hat{H})\approx\exp(-\epsilon\hat{H}^{\rm orb})\exp(\epsilon g\mu\,\hat{\boldsymbol{\sigma}}\cdot\mathbf{B}(\hat{\theta}))$, valid for small ϵ, which yields

$$\begin{aligned}&\langle\theta_j;\alpha_j|\exp(-\epsilon\hat{H})|\theta_{j-1};\alpha_{j-1}\rangle\\&\quad\approx\langle\theta_j|\exp(-\epsilon\hat{H}^{\rm orb})|\theta_{j-1}\rangle\\&\qquad\times\langle\alpha_j|\exp(\epsilon g\mu\,\hat{\boldsymbol{\sigma}}\cdot\mathbf{B}(\theta_{j-1}))|\alpha_{j-1}\rangle\,.\end{aligned} \tag{4.6}$$

We focus first on the second factor, the spin matrix element $\langle\alpha_j|\exp(\epsilon g\mu\,\hat{\boldsymbol{\sigma}}\cdot\mathbf{B}(\theta_{j-1}))|\alpha_{j-1}\rangle$. Collecting together the product of these spin matrix elements from each (imaginary) time slice, and performing the summations over intermediate spin states, one notices that for each orbital path $\{\theta_j\}$ the spin matrix elements regroup to give a single simple matrix element. In the limit that the number of slices N is large, this matrix element is then recognized to be the spin propagator,

$$\langle\alpha_f|\hat{U}_\theta(\beta)|\alpha_i\rangle=\langle\alpha_f|\,T\,e^{-\int_0^\beta d\tau\,\hat{H}^s(\tau)}\,|\alpha_i\rangle, \tag{4.7}$$

i.e., the matrix element of the (imaginary) time-ordered form of the (imaginary) time-evolution operator for the problem of a single spin-$\frac{1}{2}$ evolving according to the orbital-path–dependent Hamiltonian

$$\hat{H}^s(\tau)=-g\mu\,\mathbf{B}(\theta(\tau))\cdot\hat{\boldsymbol{\sigma}}, \tag{4.8}$$

where $\theta(\tau_j)=\theta_j$. This propagator $\hat{U}_\theta(\tau)$ satisfies the Schrödinger-Bloch equation

$$\frac{\partial}{\partial\tau}\hat{U}_\theta(\tau)=-\hat{H}^s(\tau)\,\hat{U}_\theta(\tau), \tag{4.9}$$

with initial condition $\hat{U}_\theta(0)=\hat{\mathbb{1}}$, in which $\mathbb{1}$ is the identity operator in spin space. Using this spin-orbit decomposition the full propagator $G(\theta_f,\alpha_f;\theta_i,\alpha_i)$ takes the form of an average over Feynman paths $\theta(\tau)$ weighted by the spin propagator for a spin-$\frac{1}{2}$ particle evolving in the presence of a $\theta(\tau)$-dependent magnetic field.

C. Decompactification, winding number, and orbital action

To find the precise form of the path integral, we evaluate the orbital matrix elements $\langle\theta_j|e^{-\epsilon\hat{H}^{\rm orb}}|\theta_{j-1}\rangle$ following Kleinert.[18] We introduce the periodic inner product

$$\begin{aligned}\langle\theta|\theta'\rangle&=\sum_{\nu=-\infty}^{\infty}\delta(\theta-\theta'+2\pi\nu)\\&=\sum_{\nu=-\infty}^{\infty}\int_{-\infty}^{\infty}(dp/2\pi\hbar)\,e^{ip(\theta-\theta'+2\pi\nu)/\hbar},\end{aligned} \tag{4.10}$$

thus obtaining

$$\langle\theta|e^{-\epsilon\hat{H}^{\rm orb}}|\theta'\rangle \approx e^{-\epsilon V(\theta')}\,\langle\theta|e^{-\tilde{\epsilon}\left(\hat{p}_\theta - q a \hat{A}_\theta\right)^2}|\theta'\rangle$$
$$\approx e^{-\epsilon V(\theta')}\,(1-\tilde{\epsilon}\{(-i\hbar\partial_\theta)^2 + iq\hbar[\partial_\theta A_\theta(\theta') + A_\theta(\theta)\partial_\theta] + q^2 A_\theta(\theta')^2\})\langle\theta|\theta'\rangle$$
$$\approx e^{-\epsilon V(\theta')}\sum_{\nu=-\infty}^{\infty}\int_{-\infty}^{\infty}(dp/2\pi\hbar)\,e^{ip(\theta-\theta'+2\pi\nu)/\hbar}(1-\tilde{\epsilon}\{p^2 - qp[A_\theta(\theta)+A_\theta(\theta')] + q^2 A_\theta(\theta')^2\}), \tag{4.11}$$

where $\tilde{\epsilon}\equiv\epsilon/2ma^2$. Introducing the midpoint value $\bar{A}_\theta(\theta')\equiv[A_\theta(\theta')+A_\theta(\theta)]/2$ and reexponentiating we find

$$\langle\theta|e^{-\epsilon\hat{H}^{\rm orb}}|\theta'\rangle \approx \sum_{\nu=-\infty}^{\infty}\int_{-\infty}^{\infty}(dp/2\pi\hbar)e^{ip(\theta-\theta'+2\pi\nu)/\hbar-(\epsilon/2ma^2)[p-q\bar{A}_\theta(\theta')]^2-\epsilon V(\theta')}. \tag{4.12}$$

Collecting together the orbital and spin parts, we arrive at the full thermal propagator

$$G(\theta_f,\alpha_f;\theta_i,\alpha_i)\approx\int_0^{2\pi}\prod_{j=1}^{N-1}d\theta_j\,\langle\theta_f;\alpha_f|\hat{U}_\theta(\beta)|\theta_i;\alpha_i\rangle$$
$$\times\int_{-\infty}^{\infty}\prod_{j=1}^{N}(dp_j/2\pi\hbar)$$
$$\times\sum_{\nu_1=-\infty}^{\infty}\cdots\sum_{\nu_N=-\infty}^{\infty}\exp\left(i\sum_{j=1}^{N}p_j\,(\theta_j-\theta_{j-1}+2\pi\nu_j)/\hbar\right.$$
$$\left.-\sum_{j=1}^{N}\{\tilde{\epsilon}\,[p_j-q\bar{A}_\theta(\theta_j)]^2-\epsilon V(\theta_j)\}\right). \tag{4.13}$$

We absorb the sums over integers $\{\nu_j\}$ by extending the ranges of integrations over $\{\theta_j\}$ from $(0,2\pi)$ to $(-\infty,\infty)$, using the periodicity in θ of $\bar{A}_\theta$, $\mathbf{B}$, and V, thus obtaining

$$G(\theta_f,\alpha_f;\theta_i,\alpha_i)\approx\sum_{\nu=-\infty}^{\infty}\int_{-\infty}^{\infty}\prod_{j=1}^{N-1}d\theta_j\langle\theta_f;\alpha_f|\hat{U}_\theta(\beta)|\theta_i;\alpha_i\rangle$$
$$\times\int_{-\infty}^{\infty}\prod_{j=1}^{N}(dp_j/2\pi\hbar)\exp\left(i\sum_{j=1}^{N}p_j\,(\theta_j-\theta_{j-1}+2\pi\nu\delta_{j,N})/\hbar\right.$$
$$\left.-\sum_{j=1}^{N}\{\tilde{\epsilon}[p_j-q\bar{A}_\theta(\theta_j)]^2-\epsilon V(\theta_j)\}\right) \tag{4.14}$$

In this way, we have *decompactified* the path integral, in the sense that the formerly compact variables $\{\theta_j\}$ now extend over the entire real axis. Consequently, the one remaining summation over integers ν can be interpreted as a summation over the winding numbers of the paths[16,18] $\theta(\tau)$. Next we integrate out the momenta $\{p_j\}$, yielding

$$G(\theta_f,\alpha_f;\theta_i,\alpha_i)=\sum_{\nu=-\infty}^{\infty}\int_{\theta(0)=\theta_i}^{\theta(\beta)=\theta_f+2\pi\nu}\mathcal{D}_e\theta\;e^{-S^{\rm orb}[\theta]}\;\langle\alpha_f|\hat{U}_\theta(\beta)|\alpha_i\rangle, \tag{4.15}$$

where we have passed to the limit $N\to\infty$, the subscript e on the measure indicates the *extended* nature of the paths, and the Euclidian orbital action $S^{\rm orb}[\theta]$ is given by

$$S^{\rm orb}[\theta]=\int_0^\beta d\tau\left(\frac{ma^2}{2\hbar^2}\,\dot{\theta}(\tau)^2-\frac{iaq}{\hbar}A_\theta(\theta(\tau))\,\dot{\theta}(\tau)+V(\theta(\tau))\right). \tag{4.16}$$

We note that no approximations have been made at this stage, and that the form (4.15) clearly expresses the factorization of the integrand into orbital and spin-dependent degrees of freedom.

D. Adiabatic approximation and Berry's phase

To calculate the spin matrix element $\langle\alpha_f|\hat{U}_\theta(\beta)|\alpha_i\rangle$ for an arbitrary texture, i.e., to solve the problem of the (imaginary-time) motion of a quantum-mechanical spin in the presence of the magnetic field $\mathbf{B}(\theta(\tau))$, we use the adiabatic approximation.[19,11] This approximation is valid (as we shall explicitly confirm below for the case of the cylindrically symmetric texture) provided that the Bohr frequency $\omega_B=2g\mu B/\hbar$ far exceeds the orbital frequency $\omega_o=l\Delta/\hbar$, where $\Delta=\hbar^2/2ma^2$ measures the smallest splitting of the orbital energy levels (thus setting the energy scale for the orbital aspect of the problem), l is the magnitude of the maximum (half-integral) orbital angular momentum quantum number contributing

significantly to the partition function, and B is the minimum magnitude of the magnetic field. More precisely, one needs $g\mu B/l\Delta \gg \sqrt{1-|\mathbf{N}|^2}$, where the texture-dependent vector $\mathbf{N}$ is the average of the direction of the magnetic field, and is defined in Sec. V D. The term $\sqrt{1-|\mathbf{N}|^2}$ accounts for the fact that the adiabatic approximation is exact for the trivial case of homogeneous textures (for which $|\mathbf{N}|^2=1$) regardless of the values of B and $l\Delta$. The implied physical requirement, then, is that the spin of the particle should precess around the local magnetic-field direction many times during each orbit of the particle around the ring.

In order to make the adiabatic approximation we introduce an alternative complete set of spin states $|\mathbf{B}(\theta),\alpha\rangle$ which are eigenstates of $\mathbf{B}(\theta)\cdot\hat{\boldsymbol{\sigma}}$, i.e., $\mathbf{B}(\theta)\cdot\hat{\boldsymbol{\sigma}}\,|\mathbf{B}(\theta),\alpha\rangle = \alpha B(\theta)\,|\mathbf{B}(\theta),\alpha\rangle$. Note that for each position $0\le\theta<2\pi$ such a set of states is introduced. We choose $|\mathbf{B}(\theta),\alpha\rangle$ to depend only on the direction $\mathbf{n}(\theta)=\mathbf{B}(\theta)/B(\theta)$, where $B(\theta)$ is the magnitude of the magnetic field. As stated above, we impose the physical choice that all states obey periodic boundary conditions. To obtain this, we require that both the orbital state $|\theta\rangle$ and the spin state $|\mathbf{B}(\theta),\alpha\rangle$ are periodic functions of θ. Now, $\mathbf{B}$ is a periodic function of θ. Thus, $|\mathbf{B}(\theta),\alpha\rangle$ is periodic provided that $|\mathbf{B},\alpha\rangle$ is a single-valued function of $\mathbf{B}$. Although it is not possible to construct a basis $|\mathbf{B},\alpha\rangle$ which is a single-valued function of $\mathbf{B}$ *globally* (i.e., over the entire surface of the unit sphere of magnetic-field directions $\mathbf{n}$), it *is* possible to adopt a basis which is single valued *locally* (i.e., over a texture-dependent patch on the unit sphere). More explicitly, let us consider the arbitrary texture[20]

$$\mathbf{B}(\theta)=B(\theta)\,[\sin\chi(\theta)\cos\eta(\theta)\,\mathbf{e}_x+\sin\chi(\theta)\sin\eta(\theta)\,\mathbf{e}_y+\cos\chi(\theta)\,\mathbf{e}_z] \tag{4.17}$$

in which χ and η must be chosen such that $\mathbf{B}(\theta)$ is periodic in θ, and $\{\mathbf{e}_x,\mathbf{e}_y,\mathbf{e}_z\}$ forms a Cartesian orthonormal basis. One may, e.g., choose to associate with this texture the basis of locally single-valued eigenstates

$$|\mathbf{B}(\theta),\alpha\rangle = |\alpha\rangle\,\alpha\cos\tfrac{1}{2}\chi(\theta)+|-\alpha\rangle\,e^{i\alpha\eta(\theta)}\sin\tfrac{1}{2}\chi(\theta)\,. \tag{4.18}$$

These states are not globally single valued because they are not single valued at $\chi=\pi$. We mean by this that there is more than one ket for a given value of the field, i.e., for all $\eta'\neq 0$

$$\mathbf{B}(\chi=\pi,\eta+\eta')=\mathbf{B}(\chi=\pi,\eta), \tag{4.19a}$$

$$|\mathbf{B}(\chi=\pi,\eta+\eta'),\alpha\rangle \neq |\mathbf{B}(\chi=\pi,\eta),\alpha\rangle\,. \tag{4.19b}$$

There are infinitely many other bases which may be chosen, e.g., if one wishes to consider a texture in which $\chi=\pi$ is encountered. The physical results are of course independent of the choice of basis.[21]

Following the ideas of Berry,[7] but considering *imaginary* (rather than the usual *real*) -time dynamics, we examine the evolution of instantaneous eigenstates of $\hat{H}^s(\tau)$, i.e., states which solve the instantaneous eigenproblem

$$\hat{H}^s(\tau)\,|\mathbf{B}(\theta(\tau)),\alpha\rangle = -\alpha g\mu\,B(\theta(\tau))\,|\mathbf{B}(\theta(\tau)),\alpha\rangle. \tag{4.20}$$

We then assume that a system prepared at time $\tau=0$ in a nondegenerate instantaneous eigenstate $|\mathbf{B}(\theta(0)),\alpha\rangle$ evolves, according to the Schrödinger-Bloch equation, into the instantaneous eigenstate of $\hat{H}^s(\tau)$ with the *same quantum number* α, namely $|\mathbf{B}(\theta(\tau)),\alpha\rangle$, and in the process acquires two factors, a Boltzmann factor due to Zeeman splitting, $\exp[\alpha g\mu\int_0^\tau d\tau' B(\theta(\tau'))]$, and a geometric (i.e., Berry) phase factor, $\exp[i\Gamma_\alpha(\tau)]$. The latter factor is determined through the requirement that the state $|\psi\rangle_\tau \equiv \hat{U}_\theta(\tau)\,|\mathbf{B}(\theta(0)),\alpha\rangle$ does indeed satisfy the Schrödinger-Bloch equation $\partial_\tau\,|\psi\rangle_\tau = -\hat{H}^s(\tau)\,|\psi\rangle_\tau$, in the adiabatic approximation. Thus, inserting the adiabatic ansatz

$$|\psi\rangle_\tau \approx |\mathbf{B}(\theta(\tau)),\alpha\rangle\exp\left(i\Gamma_\alpha(\tau)+\alpha g\mu\int_0^\tau d\tau' B(\theta(\tau'))\right) \tag{4.21}$$

and using the instantaneous eigenvalue equation, (4.20), one finds that

$$\partial_\tau\,\Gamma_\alpha(\tau) = i\,\langle\mathbf{B}(\theta(\tau)),\alpha|\,\partial_\tau|\mathbf{B}(\theta(\tau)),\alpha\rangle. \tag{4.22}$$

Integration for a given Feynman path $\theta(\tau)$ then gives the geometric phase

$$\Gamma_\alpha(\beta) = -\mathrm{Im}\int_0^\beta d\tau\,\langle\mathbf{B}(\theta(\tau)),\alpha|\,\partial_\tau|\mathbf{B}(\theta(\tau)),\alpha\rangle, \tag{4.23}$$

where we have used the fact that the real part of $\langle\mathbf{B}(\theta(\tau)),\alpha|\,\partial_\tau|\mathbf{B}(\theta(\tau)),\alpha\rangle$ vanishes due to normalization. Thus the spin propagator becomes

$$\langle\mathbf{B}(\theta_f),\alpha_f|\hat{U}_\theta(\beta)|\mathbf{B}(\theta_i),\alpha_i\rangle \approx \delta_{\alpha_f,\alpha_i}\exp\left(i\Gamma_{\alpha_i}(\beta)+\alpha_i\,g\mu\int_0^\beta d\tau\,B(\theta(\tau))\right). \tag{4.24}$$

The Kronecker δ expresses the fact that in the adiabatic approximation an instantaneous eigenstate with spin projection aligned along the magnetic-field direction remains an instantaneous eigenstate. With respect to the local spin quantization axis "up" and "down" spin states are not mixed, i.e., spin-flip processes are excluded. It should be noted that even though we are considering Schrödinger-Bloch (i.e., imaginary-time) dynamics, rather than the usual Schrödinger (i.e., real-time) dynamics, the geometric phase $\Gamma_\alpha(\tau)$ does indeed turn out to be a *real* number. On the other hand, the dynamical factor becomes a Boltzmann factor, growing or decaying exponentially.[22] In the real-time Berry propagator the dynamical and geometrical aspects of the evolution operator cannot be unambiguously distinguished beyond the leading-order adiabatic approximation[23]. It would be interesting to examine whether this ambiguity survives the

transformation to imaginary time dynamics.

Using the expression for $\langle \mathbf{B}(\theta_f), \alpha_f | \hat{U}_\theta(\beta) | \mathbf{B}(\theta_i), \alpha_i \rangle$, Eq. (4.24), the complete thermal propagator can thus be written as

$$G(\theta_f, \alpha_f; \theta_i, \alpha_i) \approx \sum_{\alpha=\pm 1} \langle \alpha_f | \mathbf{B}(\theta_f), \alpha \rangle \langle \mathbf{B}(\theta_i), \alpha | \alpha_i \rangle \times \sum_{\nu=-\infty}^{\infty} \int_{\theta(0)=\theta_i}^{\theta(\beta)=\theta_f+2\pi\nu} \mathcal{D}_e\theta \; e^{-S_\alpha^{\rm eff}[\theta]}, \quad (4.25a)$$

in terms of an effective action $S_\alpha^{\rm eff}[\theta]$,

$$S_\alpha^{\rm eff}[\theta] = S^{\rm orb}[\theta] - i\Gamma_\alpha(\beta) + \alpha \int_0^\beta d\tau \, g\mu \, B(\theta(\tau)) \, . \quad (4.25b)$$

At this point we mention the well-known fact that the Feynman path $\theta(\tau)$ is continuous but typically nondifferentiable. In general, this roughness induces rapid variation in $\mathbf{B}$ which causes a violation of the assumption of adiabaticity. Such an objection can be raised for any quantum-mechanical application of Berry's phase based on the adiabatic approximation, as there are, strictly speaking, no classical dynamical variables. Nevertheless, we shall assume that, as with many path integrals (see, e.g., Ref. 16, p. 39), the dominant contribution to the path integral comes from near-classical, smooth paths, and hence, that this roughness does not invalidate our final results for the persistent currents and magnetization. Indeed, as we shall show explicitly below, this assumption is certainly valid for these quantities in the case of the symmetric texture. However, there do exist physical quantities for which this assumption breaks down. This issue will be discussed in more detail in Sec. VI E.

Next comes an important step which exploits the topology of the ring. For a given path $\theta(\tau)$ we decompose the expression for the geometric phase, Eq. (4.23), into a sum of ν identical terms, one for each time the path winds around the ring, together with a term which accounts for the fact that the path is not in general closed.[24] Defining a spin-dependent geometric gauge potential

$$A_\alpha^g(\theta) = -\mathrm{Im} \, \langle \mathbf{B}(\theta), \alpha | \, \partial_\theta | \mathbf{B}(\theta), \alpha \rangle, \quad (4.26)$$

we obtain

$$\Gamma_\alpha(\beta) = \int_0^\beta d\tau \, A_\alpha^g(\theta(\tau)) \, \dot{\theta}(\tau) = \int_{\theta_i}^{\theta_f+2\pi\nu} d\theta \, A_\alpha^g(\theta), \quad (4.27)$$

where ν is the winding number defined above. At this point it is convenient to adopt a gauge in which A_α^g is constant. This can always be achieved by suitably adjusting the phases of the spin states $|\mathbf{B}(\theta), \alpha\rangle$ in the following way. First, find any set $|\mathbf{B}(\theta), \alpha\rangle$, periodic in θ, e.g., the set given in Eq. (4.18). Next, construct the *periodic* gauge parameter $\Lambda_\alpha^g(\theta) = \int_0^\theta d\theta' \, [A_\alpha^g(\theta') - \alpha\phi^g]$, where the geometric *flux* $\alpha\phi^g$ is defined by

$$\alpha\phi^g = \frac{1}{2\pi} \int_0^{2\pi} d\theta \, A_\alpha^g(\theta), \quad (4.28)$$

and we have used the fact that the right-hand side of Eq. (4.28) is proportional to α, which we confirm below[7] in Sec. V D. Then transform to a new set of spin states

$$|\mathbf{B}(\theta), \alpha\rangle \to e^{i\Lambda_\alpha^g(\theta)} \, |\mathbf{B}(\theta), \alpha\rangle \, . \quad (4.29)$$

For these states A_α^g will be independent of θ. The geometric flux ϕ^g associated with A_α^g is gauge invariant in the sense that it is invariant under $A_\alpha^g \to A_\alpha^g - \partial_\theta \tilde{\Lambda}_\alpha^g$ for any periodic gauge parameter $\tilde{\Lambda}_\alpha^g$. It can be interpreted geometrically in terms of the solid angle Ω subtended by the texture $\mathbf{B}(\theta)$ at the origin of the space of magnetic fields,[7] i.e., $\exp(2\pi i \phi^g) = \exp(-i\Omega/2)$. Thus ϕ^g represents certain geometric information about the texture. Together with some further geometric information which we shall introduce below, ϕ^g describes the physical consequence of the texture $\mathbf{B}(\theta)$ in the adiabatic limit.

In the gauge in which A_α^g is constant the geometric phase factor takes the particularly simple form

$$\exp[i\Gamma_\alpha(\beta)] = \exp[i\alpha \, (2\pi\nu + \theta_f - \theta_i) \, \phi^g] \, , \quad (4.30)$$

in which it should be noted that θ_i and θ_f are restricted to the interval $(0, 2\pi)$. Furthermore, this form for Γ_α makes explicit the fact that the only dependences it has on the path are the winding number ν and the initial and final points θ_i and θ_f. Hence Γ_α is a topological term and, as such, does not affect the classical equation of motion obtained from the effective action, Eq. (4.25b). In particular, the phase factor containing Γ_α factorizes out of the path integral for a given winding number, producing a phase factor to which only the interference terms between winding number sectors are sensitive. Finally, we note that as a consequence of the gauge transformation Eq. (4.29) the transition amplitudes in the propagator (4.25a) acquire additional phase factors.

We now briefly return to the electromagnetic gauge potential $A_\theta^{\rm em}$ to which analogous remarks apply. In particular, it is always possible to make a *periodic* gauge transformation from an arbitrary periodic gauge potential $A_\theta^{\rm em}(\theta)$ to a gauge potential which is constant on the ring and produces the same electromagnetic (dimensionless) flux $\phi^{\rm em}$. Adopting such a gauge one finds

$$\frac{qa}{\hbar} \int_0^\beta d\tau \, A_\theta^{\rm em}(\theta) \, \dot{\theta}(\tau) = (2\pi\nu + \theta_f - \theta_i) \, \phi^{\rm em}. \quad (4.31)$$

Putting all the pieces together we find that the propagator takes the form

$$G(\theta_f, \alpha_f; \theta_i, \alpha_i) \approx \sum_{\alpha=\pm 1} e^{i\Lambda_\alpha^g(\theta_f) - i\Lambda_\alpha^g(\theta_i)} \langle \alpha_f | \mathbf{B}(\theta_f), \alpha \rangle \langle \mathbf{B}(\theta_i), \alpha | \alpha_i \rangle \sum_{\nu=-\infty}^{\infty} \int_{\theta(0)=\theta_i}^{\theta(\beta)=\theta_f+2\pi\nu} \mathcal{D}_e\theta \, e^{-S_\alpha^{\rm eff}[\theta]}, \quad (4.32a)$$

$$S_\alpha^{\rm eff}[\theta] = \int_0^\beta d\tau \left(\frac{ma^2}{2\hbar^2} \, \dot{\theta}(\tau)^2 + i(2\pi\nu + \theta_f - \theta_i)\Phi_\alpha + V(\theta(\tau)) + \alpha \, g\mu B(\theta(\tau)) \right). \quad (4.32b)$$

We have introduced the total spin-dependent (dimensionless) flux Φ_α, given by

$$\Phi_\alpha = \phi^{\rm em} + \alpha\phi^g\,, \tag{4.33}$$

which combines the familiar electromagnetic contribution and the purely geometrical Berry flux. This form of the effective action makes explicit the close analogy between the geometric flux $\alpha\phi^g$ and the Aharonov-Bohm flux $\phi^{\rm em}$, and thus one should anticipate the existence of equilibrium currents caused by $\alpha\phi^g$ analogous to the conventional ones caused by $\phi^{\rm em}$. This completes our derivation of the thermal propagator for a spin-$\frac{1}{2}$ particle confined to a one-dimensional ring in the presence of an arbitrary magnetic texture, within the adiabatic approximation. The derivation presented here is, then, more general than that contained in Ref. 10, in that we are not restricted to highly symmetric textures. We note that this derivation can be readily extended to many-body problems with particle-particle interactions.

V. OBSERVABLE QUANTITIES FOR TEXTURES WITH CONSTANT MAGNITUDE |B|

A. Thermal propagator

In this section we shall use the thermal propagator in the adiabatic approximation, Eq. (4.32a), to compute the partition function, the charge current, the spin current and the magnetization. To perform explicitly the path integral derived in the preceding section, we make two simplifying assumptions: (i) that $V = 0$, and (ii) that the magnitude of the magnetic field B is independent of θ. As the decompactified (i.e., extended) path integral, Eq. (4.32a), now corresponds to free motion it can be performed exactly,[16] giving

$$G(\theta_f,\alpha_f;\theta_i,\alpha_i) \approx \sum_{\alpha=\pm1} e^{i\Lambda^g_\alpha(\theta_f)-i\Lambda^g_\alpha(\theta_i)}\langle\alpha_f|\mathbf{B}(\theta_f),\alpha\rangle\langle\mathbf{B}(\theta_i),\alpha|\alpha_i\rangle$$
$$\times\exp[\alpha\beta g\mu B + i(\theta_f-\theta_i)\Phi_\alpha - \kappa^2(\theta_f-\theta_i)^2/2]\sqrt{\kappa^2/2\pi}\,\vartheta_3[\pi\Phi_\alpha + \pi i\kappa^2(\theta_f-\theta_i); 2\pi i\kappa^2], \tag{5.1}$$

where $\kappa^2 = ma^2/\beta\hbar^2$ is a dimensionless parameter which measures the ratio of the thermal energy and the spacing between low-lying energy levels for a free particle on the ring. For a ring of radius 3000 Å and a temperature of 10 mK, κ is of order unity. In addition we have introduced the Jacobi θ function[25] $\vartheta_3(z;t) = \sum_{\nu=-\infty}^{\infty}\exp\left(i\pi t\nu^2 + 2i\nu z\right)$.

B. Canonical partition function

Using $\vartheta_3(z;t) = (-it)^{-1/2}\exp(z^2/i\pi t)\,\vartheta_3(z/t\,;-1/t)$, an identity which follows from the Poisson summation formula,[16] we find that the partition function becomes

$$Z = \sum_{\alpha=\pm1}\int_0^{2\pi} d\theta\, G(\theta,\alpha;\theta,\alpha), \tag{5.2a}$$

$$\approx \sqrt{2\pi}\,\kappa \sum_{\alpha=\pm1} e^{\alpha\beta g\mu B}\,\vartheta_3\left(\pi\Phi_\alpha; 2\pi i\kappa^2\right), \tag{5.2b}$$

$$= \sum_{\alpha=\pm1}\sum_{n=-\infty}^{\infty} e^{-\beta\mathcal{E}_{n,\alpha}}, \tag{5.2c}$$

where the effective single-particle energy spectrum is given by

$$\mathcal{E}_{n,\alpha} = \frac{\hbar^2}{2ma^2}(n-\Phi_\alpha)^2 - \alpha g\mu B\,. \tag{5.3}$$

Whereas the integral summation index ν refers to winding numbers of real-space trajectories, the index n refers to the associated orbital angular momentum quantum numbers. Earlier, in Sec. IV D, we saw that the Lagrangean framework led to the interpretation of the geometric flux as a spin-dependent gauge potential. Now, within an effective Hamiltonian framework, we see this interpretation once again, with the gauge potential occurring explicitly in the spectrum.[26]

C. Charge current

From the definition of the charge current, Eq. (3.1), one can see that it can exactly be obtained as the derivative of the partition function with respect to the electromagnetic flux $\phi^{\rm em}$. Using the adiabatic approximation for the partition function, Eq. (5.2c), we find

$$\langle\hat{J}^0\rangle = \kappa^2\frac{\partial}{\partial\phi^{\rm em}}\ln Z \approx \frac{1}{Z}\sum_{n,\alpha}(n-\Phi_\alpha)\,e^{-\beta\mathcal{E}_{n,\alpha}}. \tag{5.4}$$

This current is a manifestly periodic function of $\phi^{\rm em}$ and ϕ^g, with period unity, vanishing whenever $2\Phi_\pm$ are both integral. Figure 2 shows the dependence of the charge current on $\phi^{\rm em}$ and ϕ^g at low but nonzero temperature.

Next we examine the charge current in the low-temperature limit. As in this limit $\beta g\mu B \gg 1$, we need only retain terms with $\alpha = 1$. Furthermore, it is convenient to use the propagator expressed in terms of ϑ_3, and to make use of the result[27]

$$\partial_z\ln\vartheta_3(z;t) = 4\sum_{\nu=1}^{\infty}\frac{(-q)^\nu}{1-q^{2\nu}}\sin(2\nu z)\,, \tag{5.5}$$

where $q = \exp i\pi t$. As $t = 2\pi i\kappa^2$ the denominator $(1-q^{2\nu})$ becomes $(2\pi\kappa)^2\nu + O(\kappa^4)$, for $\kappa \to 0$. Thus, in the low-temperature limit and in the adiabatic approximation the charge current is given by the saw-tooth function

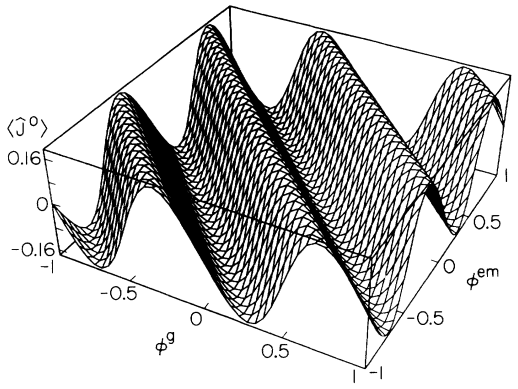

FIG. 2. The (dimensionless) charge current $\langle \hat{J}^0 \rangle$ as a function of the electromagnetic flux $\phi^{\rm em}$ and the geometric flux ϕ^g at temperature $T = 1$ mK for a ring of radius $a = 3000$ Å and for a magnetic field of magnitude $B = 50$ G.

$$\langle \hat{J}^0 \rangle \to \langle \hat{J}^0 \rangle_0 \approx \frac{1}{\pi} \sum_{\nu=1}^{\infty} \frac{(-1)^\nu}{\nu} \sin(2\pi\nu\Phi_+) = -\Phi_+ , \tag{5.6}$$

where the last equality holds for $-\frac{1}{2} < \Phi_+ < \frac{1}{2}$. At the end points $\Phi_+ = \pm\frac{1}{2}$ of this interval the current is zero, and for values of Φ_+ outside this interval the current should be periodically extended. Of course this result, Eq. (5.6), also follows directly from Eq. (5.4). However the summation form in Eq. (5.6) clearly exhibits the periodicity in Φ_+ and demonstrates that all winding numbers contribute at $T = 0$. Figure 3 shows the dependence of the charge current on $\phi^{\rm em}$ and ϕ^g at zero temperature.

We mention that in cases dominated by either $\alpha = 1$ or -1 the electromagnetic flux $\phi^{\rm em}$ is simply augmented by the geometric flux $\alpha\phi^g$. As a consequence, the oscillation of the conventional persistent charge current with respect to electromagnetic flux is offset by a shift which is geometric in origin. We further mention that in the case of degenerate Fermi systems, where both $\alpha = 1$ and -1 contribute, such an offset also occurs, as we plan to discuss in detail in a forthcoming paper.[9]

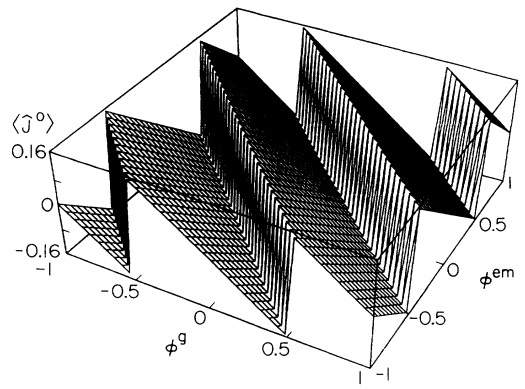

FIG. 3. The zero-temperature (dimensionless) charge current $\langle \hat{J}^0 \rangle_0$ as a function of the electromagnetic flux $\phi^{\rm em}$ and the geometric flux ϕ^g.

D. Spin current

To compute the equilibrium expectation value of the three Cartesian components $\langle \hat{J}^k \rangle$ of the spin current, we apply Eq. (4.3) and use the thermal propagator given in Eq. (5.1). Standard manipulations, involving the periodic matrix element

$$\langle \theta | \hat{p}_\theta | \theta' \rangle = -i\hbar\partial_\theta \langle \theta | \theta' \rangle = -i\hbar\partial_\theta \sum_{\nu=-\infty}^{\infty} \delta(\theta - \theta' + 2\pi\nu) \tag{5.7}$$

and integrations by parts (in which periodicity eliminates the boundary contributions), produce the following expression for the spin current:

$$\langle \hat{\mathbf{J}} \rangle \approx \frac{\sqrt{2\pi}\kappa}{Z} \sum_\alpha e^{\alpha\beta g\mu B} \left(\mathbf{F}\, \vartheta_3(\pi\Phi_\alpha; 2\pi i\kappa^2) + \mathbf{N}\,\kappa^2 \frac{\partial}{\partial\phi^g} \vartheta_3(\pi\Phi_\alpha; 2\pi i\kappa^2) \right), \tag{5.8a}$$

$$\mathbf{F} = \frac{1}{2\pi} \int_0^{2\pi} d\theta \,[\, (i\,\partial_\theta \langle \mathbf{B}(\theta), \alpha |)\, \hat{\boldsymbol{\sigma}} | \mathbf{B}(\theta), \alpha \rangle - \mathrm{Im}\, \langle \mathbf{B}(\theta), \alpha | \hat{\boldsymbol{\sigma}} | \mathbf{B}(\theta), \alpha \rangle \times \langle \mathbf{B}(\theta), \alpha | \partial_\theta | \mathbf{B}(\theta), \alpha \rangle \,], \tag{5.8b}$$

$$\mathbf{N} = \frac{\alpha}{2\pi} \int_0^{2\pi} d\theta\, \langle \mathbf{B}(\theta), \alpha | \hat{\boldsymbol{\sigma}} | \mathbf{B}(\theta), \alpha \rangle . \tag{5.8c}$$

Direct evaluation of $\mathbf{F}$ and $\mathbf{N}$ using the explicit form of the matrix elements given in Eq. (4.18) shows that they are indeed independent of α and real, and are given in terms of the texture by the compact averages

$$\mathbf{F} = -\frac{1}{4\pi} \int_0^{2\pi} d\theta\, \mathbf{n}(\theta) \wedge \partial_\theta \mathbf{n}(\theta), \tag{5.9a}$$

$$\mathbf{N} = \frac{1}{2\pi} \int_0^{2\pi} d\theta\, \mathbf{n}(\theta), \tag{5.9b}$$

where $\mathbf{n} = \mathbf{B}/B$, and where $\wedge$ denotes the usual vector product. In terms of these simple averages of the texture the spin current takes the final form[28]

$$\langle \hat{\mathbf{J}} \rangle \approx \mathbf{F} + \mathbf{N}\,\kappa^2 \frac{\partial}{\partial\phi^g} \ln Z, \tag{5.10}$$

$$= \mathbf{F} + \mathbf{N}\,\frac{1}{Z} \sum_{\alpha,n} \alpha(n - \Phi_\alpha)\, e^{-\beta\mathcal{E}_{n,\alpha}} . \tag{5.11}$$

This current is also periodic in $\phi^{\rm em}$ and ϕ^g with period unity, vanishing when $2\phi^{\rm em}$ and ϕ^g are both integral (as should become clearer from the following discussion of $\mathbf{F}$).

The texture-dependent quantities $\mathbf{F}$ and $\mathbf{N}$ have simple

interpretations. The latter is simply the mean value of the unit vector $\mathbf{n}$ pointing in the direction of the magnetic field. As such, it is *not* a purely geometrical quantity; textures which visit identical collections of values of the magnetic field do not necessarily give identical values of $\mathbf{N}$. In other words, the textures $\mathbf{B}(\theta)$ and $\mathbf{B}(f(\theta))$ (with f being a reparametrization) do not necessarily give rise to the same $\mathbf{N}$. On the other hand, $\mathbf{F}$ *is* purely geometrical, as can be seen by rewriting it as

$$\mathbf{F} = -\frac{1}{4\pi}\int_{C=\partial\Sigma} \mathbf{n}\wedge d\mathbf{n} = -\frac{1}{2\pi}\int_{\Sigma} d\mathbf{S}, \tag{5.12}$$

where the surface Σ lies on the unit sphere and has the closed curve C as its boundary,[29] and we have made use of the (vector) Stokes theorem. The element $d\mathbf{S}$ is the outward normal surface element which becomes $\mathbf{n}\,d\Omega$ on the surface of the unit sphere, where $d\Omega$ is the surface area element. The surface integral representation shows that the kth component of the *geometric vector* F^k can be interpreted (up to a constant factor) as the area of the projection on to the plane orthogonal to the kth coordinate axis of the surface Σ, as shown in Fig. 4. (See also Ref. 30.) Alternatively, F^k can be interpreted as the flux through Σ of a uniform vector field $\mathbf{V} = \mathbf{e}^k$.

In contrast, the Berry flux, which is also a geometrical object, is simply the *area* (rather than the *projected* area) of the surface Σ, and is given by

$$\phi^g = -\frac{1}{4\pi}\int_{\Sigma} d\mathbf{S}\cdot\mathbf{n} = \frac{1}{4\pi}\int_0^{2\pi} d\theta\,[\cos\chi(\theta)-1]\,\partial_\theta\eta(\theta)\,, \tag{5.13}$$

where the last expression follows from Eqs. (4.18) and (4.28). Alternatively, ϕ^g can be interpreted as the flux of the vector field $\mathbf{V} = \mathbf{n}$ ($= \mathbf{B}/B^3$ on the unit sphere) through the surface Σ, i.e., the flux through Σ due to a fictitious monopole located at the center of the sphere.[7] It should be noted that the geometric vector $\mathbf{F}$ provides information about the geometry of the texture which is *independent* of that provided by the geometric phase. One can see this by noting that it is possible to change the texture in such a way that ϕ^g changes but $\mathbf{F}$ does not. In addition, it is worthwhile introducing a natural extension of the Berry flux, $\phi^g(\mathbf{x})$, obtained by locating the monopole not at the center of the sphere but instead at the position $\mathbf{x}$. Then

$$\phi^g(\mathbf{x}) = -\frac{1}{4\pi}\int_{\Sigma}\frac{d\mathbf{S}\cdot\mathbf{n}}{|\mathbf{x}-\mathbf{n}|}, \tag{5.14}$$

so that $\phi^g = \phi^g(\mathbf{x}=\mathbf{0})$ and $\mathbf{F} = \frac{1}{2}(\nabla\phi^g(\mathbf{x}))(\mathbf{x}=\mathbf{0})$. Thus the Berry flux and (twice) the geometric vector are the zeroth- and first-order coefficients in the Taylor

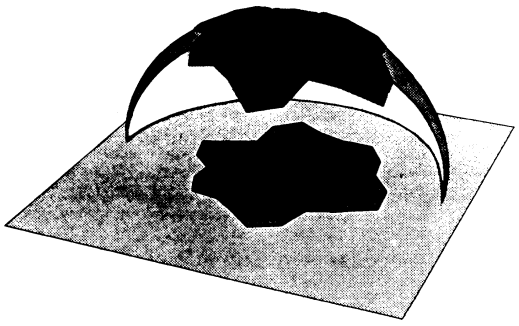

FIG. 4. Geometrical interpretation of the flux ϕ^g and the vector $\mathbf{F}$. The geometric flux corresponds to the area of the shaded part of the spherical surface Σ. The component F^3 of the geometric vector corresponds to the area of the shaded part of the equatorial plane, i.e., to the area of the projection of Σ on to the equatorial plane.

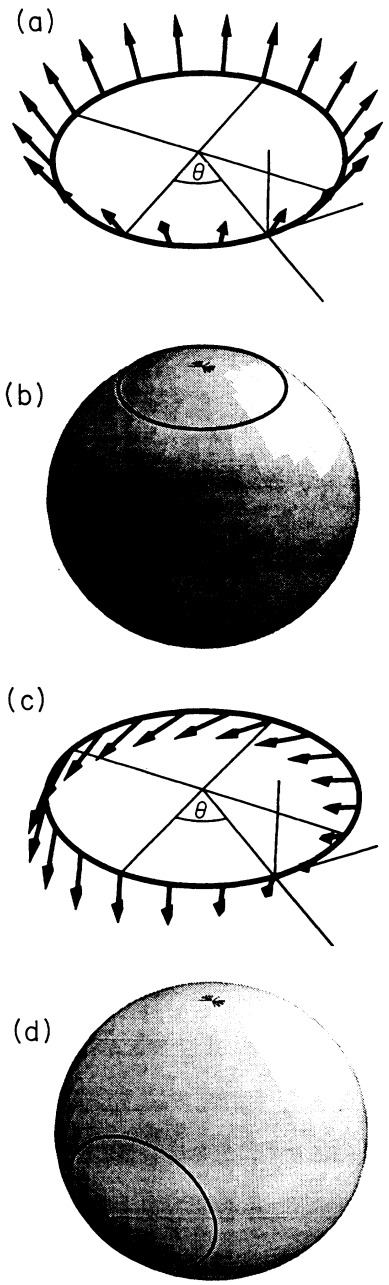

FIG. 5. Two textures related by a global rotation, each represented in two ways: (i) as the magnetic field around a ring [(a) and (c)], and (ii) as trajectories on the unit sphere [(b) and (d)].

expansion of $\phi^g(\mathbf{x})$ about $\mathbf{x} = \mathbf{0}$. It would be interesting to find physical realizations of the second- and higher-order coefficients in this series.

Yet another interpretation of the geometric vector $\mathbf{F}$ can be given using an analogy with the Biot-Savart law.[31] First, introduce a fictitious current I flowing along a closed real-space path $\mathcal{C}_d$ prescribed by $\mathbf{x}(\theta) = \mathbf{n}(\theta)\, d$ which lies on the surface of a sphere of radius d. This path is specified by the texture through $\mathbf{n}(\theta)$. Then the fictitious magnetic field $\mathbf{H}$ produced at the center of this sphere by the current loop is given by $\mathbf{H} = -(\mu_0 I/d)\mathbf{F}$.

Finally, in the low-temperature limit the spin current acquires the particularly simple form

$$\langle \hat{\mathbf{J}} \rangle \to \langle \hat{\mathbf{J}} \rangle_0 \approx \mathbf{F} + \langle \hat{J}^0 \rangle_0 \, \mathbf{N}\,, \tag{5.15}$$

where the low-temperature limit of the charge current $\langle \hat{J}^0 \rangle_0$ is given in Eq. (5.6). This result follows from Eqs. (5.11) and (5.4) upon retention only of terms with $\alpha = 1$.

E. Magnetization

To compute the equilibrium expectation value of the magnetization $\langle \hat{\boldsymbol{\sigma}} \rangle$ we again apply Eqs. (4.3) and (5.1), now obtaining

$$\langle \hat{\boldsymbol{\sigma}} \rangle \approx \mathbf{N} \frac{1}{Z} \sum_{\alpha,n} \alpha e^{-\beta \mathcal{E}_{n,\alpha}}. \tag{5.16}$$

In the low-temperature limit the magnetization is given by

$$\langle \hat{\boldsymbol{\sigma}} \rangle \to \langle \hat{\boldsymbol{\sigma}} \rangle_0 \approx \mathbf{N}. \tag{5.17}$$

Equations (5.9a), (5.9b), (5.13), and (5.10) show that for textures related by a global (i.e., θ-independent) rotation the corresponding spin currents are related by the same rotation, and similarly for the magnetizations. This, of course, is a reflection of the vector character of the operators $\hat{\mathbf{J}}$ and $\hat{\boldsymbol{\sigma}}$. Two textures related by such a global rotation are depicted in Fig. 5.

F. Quantum correlations and interpretation

The spin current $\langle \hat{\mathbf{J}} \rangle$ provides a useful tool for examining the origin of the quantum-mechanical correlations at low temperatures. In particular, we now show that the geometric vector $\mathbf{F}$ lends itself to an interpretation *precisely* in terms of these correlations. To see this, we notice that the spin current can be written as[28] $\langle \hat{\mathbf{J}} \rangle = \langle J^0 \hat{\boldsymbol{\sigma}} \rangle$. Then, using Eqs. (5.15) and (5.17), it follows that in the low-temperature limit

$$\langle J^0 \hat{\boldsymbol{\sigma}} \rangle_0 - \langle J^0 \rangle_0 \langle \hat{\boldsymbol{\sigma}} \rangle_0 \approx \mathbf{F}\,. \tag{5.18}$$

Clearly the geometric vector represents the quantum-mechanical correlation between the orbital and spin degrees of freedom. Thus, Eq. (5.18) reveals the existence of an effective coupling between orbital and spin motion induced by the geometry of the texture.

The notion of spin-orbit coupling provides a useful heuristic picture of the processes responsible for persistent charge currents in the absence of an electromagnetic flux ϕ^{em}. First, consider the case in which the texture gives a nonzero value of $\mathbf{N}$. Then, by Eq. (5.17), the spin is polarized, i.e., there is a nonzero magnetization and, through the coupling between spin and orbital motion, the orbital angular momentum can acquire a nonzero expectation value. In other words, as a consequence of the geometric phase — a purely quantum-mechanical object — one sense of orbital motion can become energetically preferred over the other. As the particles carry charge, the system would then exhibit an equilibrium charge current. On the other hand, the spin current is simply a measure of the correlation between spin and orbital motion reflecting the coupling between them.

Second, consider the case in which the texture gives a vanishing value of $\mathbf{N}$. In this case the spin is unpolarized, i.e., the magnetization is zero. Despite this, the spin and orbital motion are still coupled through the geometric phase and thus the quantum fluctuations in spin and orbital angular momentum are correlated. For example, fluctuations which produce a positive z component of spin and a negative z component of orbital angular momentum (or vice versa) give a larger contribution to the partition function than those with parallel z components. Hence, their product — the spin current — is typically negative. On the other hand, in the absence of a magnetization there is nothing to bias the orientation of the orbital angular momentum fluctuations and thus there will be no charge current.

One should not take this picture too literally: as $\mathbf{F}$, $\mathbf{N}$, and ϕ^g are independent one can construct textures for which the magnetization vanishes and yet there is a nonzero charge current, and vice versa. For example, the texture obtained by reparametrizing the cylindrically symmetric planar texture, i.e., $\chi = \pi/2$ and $\eta = \theta - \sin\theta$, gives $\phi^g = -\frac{1}{2}$ and $\mathbf{N} \neq \mathbf{0}$. Thus this texture produces a magnetization but no charge current.

That our effective spin-orbit coupling and spin currents are essentially equivalent can be envisaged in the following way, as suggested by Goeppert-Meyer. Consider a pair of dancers performing a Viennese waltz around a ballroom. As they orbit around the dance floor they also spin about their center of mass. Typically they spin in the sense opposite to their orbital angular momentum.

Finally we remark that the persistent currents described here vanish in the limit that the ring becomes large. This can be seen from the normalization of the physical (i.e., dimensionful) currents given at the beginning of Sec. III. Considering M noninteracting and nondegenerate particles on the ring, we find the charge (or spin) current to be proportional to $Mq\hbar/ma^2$ (or $M\hbar^2/ma^2$). In the thermodynamic limit, i.e., $M, a \to \infty$ with constant density $M/2\pi a$, the currents vanish. Thus, we regard these currents as *mesoscopic* phenomena.[14] Furthermore, the electromagnetic fields which these currents produce vanish in the classical limit $\hbar \to 0$; thus they are purely quantum mechanical in origin. On general grounds it is clear that the currents also vanish in the high-temperature limit. However, whereas the charge current calculated using our adiabatic approxi-

mation does vanish in the high-temperature limit, we do not find that the spin current vanishes in this limit, due to the temperature-independent geometric vector **F**. No significance should be attached to this result because the realm of validity of the adiabatic approximation does not include high temperatures ($\omega_O > \omega_B$) and hence its predictions are untrustworthy for them.

Similarly, one might expect that these quantum-mechanical persistent currents should vanish if calculated using a thermal propagator from which contributions due to paths with nonzero winding number have been omitted. The reason is that the effective action of Feynman paths which do not wind around the ring is independent of electromagnetic or geometric flux. Indeed, we find that in this case the charge current vanishes, but that the spin current does not, once again due to the presence of the geometric vector. Similarly, no significance should be attached to this result because the realm of validity of the adiabatic approximation does not include $\omega_O > \omega_B$, i.e., large angular momenta, and hence its predictions are untrustworthy for small winding numbers.

G. Symmetric textures in the adiabatic approximation

In Sec. VI we shall compute observable quantities for the case of cylindrically symmetric textures by exactly solving the time-independent Schrödinger equation. Here, we collect the results of the path-integral adiabatic approximation for such textures so that they may be compared with the exact results presented below.

Cylindrically symmetric textures are those which can be written in the form

$$\mathbf{B}(\theta) = B\,(\mathbf{e}_z \cos\chi + \mathbf{e}_r \sin\chi)\ , \tag{5.19}$$

or can obtained from such a form by a global (i.e., θ-independent) rotation of $\mathbf{B}(\theta)$. Here, $\{\mathbf{e}_r, \mathbf{e}_\theta, \mathbf{e}_z\}$ forms an orthonormal basis for a cylindrical polar coordinate system on the ring, and the texture is then parametrized by the magnitude of the field B and the tilt angle χ (i.e., the angle by which the texture departs from the vertical direction). Figure 6 depicts a cylindrically symmetric *crown-shaped* texture. This form can be obtained from the arbitrary texture, Eq. (4.17), by choosing $\chi(\theta) = \chi$ (a constant) and $\eta(\theta) = \theta$.

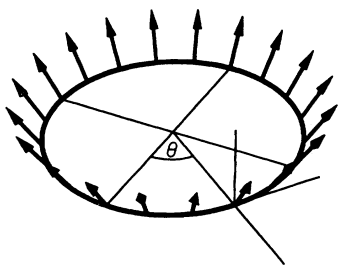

FIG. 6. Mesoscopic ring (thick circle) in a cylindrically symmetric *crown-shaped* inhomogeneous magnetic field (arrows) with constant tilt angle χ.

Thus, for the case of cylindrically symmetric textures the partition function and the charge current are given by Eqs. (5.2c) and (5.4), respectively, the only simplification being that the geometric phase reduces to

$$\phi^g = \tfrac{1}{2}(\cos\chi - 1). \tag{5.20}$$

Note also that Eq. (5.2c) reduces to the exact partition function when the tilt angle χ vanishes. Similarly, the low-temperature limit of the charge current is given by Eq. (5.6), with the value of ϕ^g obtained from Eq. (5.20). These results have been given in Ref. 10 (see Ref. 32).

To calculate the spin current for cylindrically symmetric textures we first compute the texture-dependent vectors **F** and **N** using Eqs. (5.9a) and (5.9b), thus obtaining

$$\mathbf{F} = -\tfrac{1}{2}\mathbf{e}_z \sin^2\chi\,, \tag{5.21a}$$

$$\mathbf{N} = \mathbf{e}_z \cos\chi\,. \tag{5.21b}$$

This leads to expressions for the components of the spin current and magnetization given in Ref. 10, i.e.,

$$\langle \hat{J}^3 \rangle \approx -\tfrac{1}{2}\sin^2\chi + \frac{1}{Z}\cos\chi \sum_{\alpha,n} \alpha(n - \Phi_\alpha)\, e^{-\beta\mathcal{E}_{n,\alpha}}\,, \tag{5.22}$$

with the other components $\langle \hat{J}^1 \rangle$ and $\langle \hat{J}^2 \rangle$ vanishing. Figure 7 shows the dependence of the spin current $\langle \hat{J}^3 \rangle$ on $\phi^{\rm em}$ and χ at low but nonzero temperature for the case of the symmetric texture. Similarly, the magnetization is given by

$$\langle \hat{\sigma}^3 \rangle \approx \frac{1}{Z}\cos\chi \sum_{\alpha,n} \alpha\, e^{-\beta\mathcal{E}_{n,\alpha}}\,. \tag{5.23}$$

This concludes the calculation of physical quantities based on the path-integral adiabatic approximation. We now turn to the particular class of textures, considered in the present subsection within the path-integral adiabatic approximation, for which exact results are independently available.

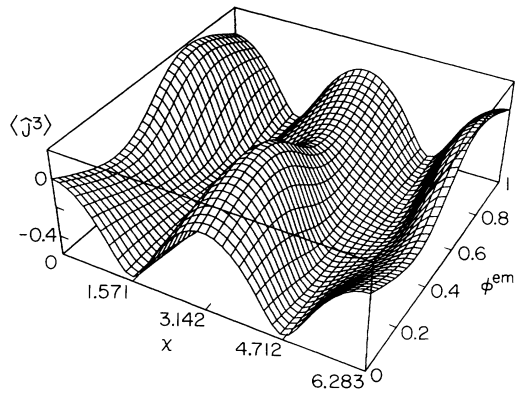

FIG. 7. The (dimensionless) spin current $\langle \hat{J}^3 \rangle$ as a function of the electromagnetic flux $\phi^{\rm em}$ and the tilt angle χ for the case of the symmetric texture at temperature $T = 1$ mK for a ring of radius $a = 3000$ Å and for a magnetic field of magnitude $B = 50$ G.

VI. EXACT SOLUTION FOR SYMMETRIC TEXTURES

So far, we have developed an approximate path-integral method which allows us to deal with arbitrary textures. Instead, we now turn to a direct approach via the solution of the time-independent Schrödinger equation. While this approach is generally intractable, the very special case of a cylindrically symmetric texture is readily solvable. By following this scheme we are able to confirm independently the validity of the path-integral approach in the adiabatic limit.

A. Symmetric model with source terms

In this subsection we consider symmetric textures and solve the model described by Eq. (2.1) in the sense that we obtain the exact spectrum of energy eigenvalues. The solution for this spectrum is due to Kuratsuji and Iida.[15]

We then use this information to compute the partition function, and derive from it the charge current, spin current, and magnetization. We achieve this via the introduction of suitable source terms which allow us to avoid the computation of eigenfunctions and matrix elements. To this end we consider the Hamiltonian

$$\hat{H} = \frac{1}{2ma^2}\left(\hat{p}_\theta - \hbar\phi^{\rm em} - \hbar\xi\hat{\sigma}^3\right)^2 - g\mu\mathbf{B}(\hat{\theta})\cdot\hat{\boldsymbol{\sigma}} - \zeta g\mu B\hat{\sigma}^3 , \tag{6.1}$$

i.e., Eq. (2.1) without the potential term $V(\theta)$ (to produce cylindrical symmetry), with the symmetric texture given in Eq. (5.19), and with source terms $\hbar\xi\hat{\sigma}^3$ to generate the spin current and $\zeta g\mu B\hat{\sigma}^3$ to generate the magnetization. The components $k = 1, 2$ of the spin current and magnetization vanish due to rotational invariance; thus, no source terms are needed to generate them. The Longuet-Higgins model of Jahn-Teller molecules bears a formal resemblance to the present model, Eq. (6.1), but of course describes a quite different physical system.[33]

B. Eigenvalue spectrum for symmetric textures

The aim is now to find the exact eigenvalues of the Hamiltonian (6.1), i.e., we must address the energy eigenproblem $\hat{H}|\psi\rangle = E|\psi\rangle$ for the Hamiltonian given in Eq. (6.1) with a Zeeman term which is proportional to

$$\hat{\sigma}\cdot\mathbf{B}(\hat{\theta}) + \zeta\hat{\sigma}^3 B = B\left[\hat{\sigma}^1\cos\hat{\theta}\sin\chi + \hat{\sigma}^2\sin\hat{\theta}\sin\chi + \hat{\sigma}^3(\zeta + \cos\chi)\right]. \tag{6.2}$$

Following Kuratsuji and Iida,[15] the solution of this problem is elementary, due to the conservation of the z component of the total angular momentum $\hat{L}^3 = \hat{p}_\theta + (\hbar/2)\hat{\sigma}^3$, where $\hat{p}_\theta$ is the orbital angular momentum, which follows from the rotational invariance about the z axis. Thus, it is convenient to work in the basis of simultaneous eigenkets of $\hat{L}^3$ and $\hat{\sigma}^3$, namely

$$\hat{L}^3|l;\aleph\rangle = \hbar l\,|l;\aleph\rangle, \tag{6.3a}$$

$$\hat{\sigma}^3|l;\aleph\rangle = \aleph\,|l;\aleph\rangle, \tag{6.3b}$$

where $l = \pm 1/2, \pm 3/2, \ldots$ and $\aleph = \pm 1$. We shall also use the basis $|\theta;\aleph\rangle$ given in Eq. (4.1), with the corresponding wave functions

$$\langle\theta;\aleph|l;\aleph'\rangle = \frac{1}{\sqrt{2\pi}}\,\delta_{\aleph,\aleph'}\,e^{i(l-\aleph/2)\theta}. \tag{6.4}$$

Note that the total angular momentum quantum number l is half-integral; this follows from the addition of an orbital and a spin angular momentum, the former being integral, by virtue of the single-valuedness (under $\theta \to \theta + 2\pi$) of the wave functions, and the latter being half-integral.

In the $\{|l;\aleph\rangle\}$ basis the matrix elements of the Hamiltonian are given by

$$\langle l;\aleph|\hat{H}|l';\aleph'\rangle = \delta_{l,l'}\,\Delta\begin{pmatrix} \ell_-^2 - b(\zeta+\cos\chi) & -b\sin\chi \\ -b\sin\chi & \ell_+^2 + b(\zeta+\cos\chi)\end{pmatrix}, \tag{6.5}$$

where $\ell_\pm = (l \pm 1/2 - \phi^{\rm em} \pm \xi)$, where $\Delta = \hbar^2/2ma^2$ has been defined at the beginning of Sec. IV D, and where $b = g\mu B/\Delta$ is the dimensionless magnetic field. The exact energy eigenvalues are then readily found to be

$$E_{l,\alpha}(\xi,\zeta) = \Delta\left\{(l-\phi^{\rm em})^2 + \tfrac{1}{4}(1+2\xi)^2 - \alpha\sqrt{[(l-\phi^{\rm em})(1+2\xi) + b(\zeta+\cos\chi)]^2 + b^2\sin^2\chi}\,\right\}, \tag{6.6}$$

where $\alpha = \pm 1$. We emphasize that this exact solution can be obtained only for highly symmetric textures, such as the cylindrically symmetric one considered here. Below, we shall discuss various limiting cases of this exact solution, in order to make contact with the path-integral solution and to discuss the validity of the adiabatic approximation.

C. Partition function, charge and spin currents, and magnetization

We now use the exact spectrum, Eq. (6.6), to compute the partition function for a single particle, from which we can construct exact expressions for the equilibrium charge and spin currents. In the presence of the source terms the canonical partition function is given by

$$Z(\xi,\zeta)=\sum_{l=\pm 1/2,\pm 3/2,\ldots}\sum_{\alpha=\pm 1} e^{-\beta E_{l,\alpha}(\xi,\zeta)} \tag{6.7a}$$

$$=2\,e^{-\beta\Delta(1+2\xi)^2/4}\sum_{l=\pm 1/2,\pm 3/2,\ldots} e^{-\beta\Delta(l-\phi^{\rm em})^2}\cosh\sqrt{[(l-\phi^{\rm em})(1+2\xi)+b(\zeta+\cos\chi)]^2+b^2\sin^2\chi}. \tag{6.7b}$$

To compute the charge current we use the expression given above in Eq. (5.4) and obtain

$$\langle J^0\rangle=-\frac{1}{2\Delta Z}\sum_{l,\alpha}\frac{\partial E_{l,\alpha}}{\partial\phi^{\rm em}}e^{-\beta E_{l,\alpha}}, \tag{6.8}$$

in which the energy spectrum follows from Eq. (6.6) as $E_{l,\alpha}=E_{l,\alpha}(\xi=0,\zeta=0)$, the partition function is given by $Z=Z(\xi=0,\zeta=0)$, and the derivative is explicitly given by

$$\partial_{\phi^{\rm em}}E_{l,\alpha}=-\Delta\left(2(l-\phi^{\rm em})-\frac{\alpha\,(l-\phi^{\rm em}+b\cos\chi)}{\sqrt{(l-\phi^{\rm em}+b\cos\chi)^2+b^2\sin^2\chi}}\right). \tag{6.9}$$

The spin current is obtained by taking the derivative with respect to ξ, giving

$$\langle J^3\rangle=(2\beta\Delta)^{-1}\partial_\xi\ln Z(\xi,0)\big|_{\xi=0}$$
$$=-(2\Delta Z)^{-1}\sum_{l,\alpha}\partial_\xi E_{l,\alpha}(\xi,0)\big|_{\xi=0}e^{-\beta E_{l,\alpha}}, \tag{6.10}$$

where

$$\partial_\xi E_{l,\alpha}(\xi,0)\big|_{\xi=0}=\Delta\left\{1-\frac{2\alpha\,(l-\phi^{\rm em})\,(l-\phi^{\rm em}+b\cos\chi)}{\sqrt{(l-\phi^{\rm em}+b\cos\chi)^2+b^2\sin^2\chi}}\right\}, \tag{6.11}$$

with the other two components vanishing by symmetry.

The magnetization is given by

$$\langle\hat\sigma^3\rangle=(\beta g\mu B)^{-1}\partial_\zeta\ln Z(0,\zeta)\big|_{\zeta=0}$$
$$=-(g\mu B\,Z)^{-1}\sum_{l,\alpha}\partial_\zeta E_{l,\alpha}(0,\zeta)\big|_{\zeta=0}e^{-\beta E_{l,\alpha}}, \tag{6.12}$$

where

$$\partial_\zeta E_{l,\alpha}(0,\zeta)\big|_{\zeta=0}=-\frac{\alpha g\mu B\,(l-\phi^{\rm em}+b\cos\chi)}{\sqrt{(l-\phi^{\rm em}+b\cos\chi)^2+b^2\sin^2\chi}}, \tag{6.13}$$

with the other two components vanishing by symmetry.

D. The planar texture

For the sake of illustration we now give the results of the exact solution for the case of the planar symmetric texture, for which $\chi=\pi/2$, under the restriction that $\phi^{\rm em}$ is integral. Under these conditions the spectrum takes the simple form

$$E_{l,\alpha}=\Delta\left(l^2+1/4-\alpha\sqrt{l^2+b^2}\right), \tag{6.14}$$

and thus the charge current and the magnetization can be seen to vanish for all temperatures, using Eqs. (6.8) and (6.9), and Eqs. (6.12) and (6.13). The charge current and the magnetization also vanish for this texture in the path-integral adiabatic approximation, as follows from Eqs. (5.4) and (5.22).

On the other hand, the spin current does not vanish for this texture (and electromagnetic flux) and is given by

$$\langle\hat J^3\rangle=\frac{1}{2Z}\sum_{l,\alpha}\left(\frac{2l^2\alpha}{\sqrt{l^2+b^2}}-1\right)e^{-\beta E_{l,\alpha}}. \tag{6.15}$$

In the low-temperature limit the spin current becomes

$$\langle\hat J^3\rangle_0=\frac{1}{2}\left(-1+\frac{1}{\sqrt{1+4b^2}}\right). \tag{6.16}$$

Now, the adiabatic limit is independent of the low-temperature limit. If, additionally, we take the adiabatic limit (which at low temperatures reads $b\gg 1$; see Sec. VI E), then Eq. (6.16) reduces to $\langle\hat J^3\rangle_0\approx-\frac{1}{2}$, i.e., precisely to the result found from the path-integral approach, Eq. (5.22), applied to the planar texture.

E. Equivalence of the exact diagonalization and path-integral approaches in the adiabatic limit

The path-integral approach to the investigation of persistent currents using the adiabatic approximation has the virtue of being able to handle arbitrary textures. On the other hand, the analysis of cylindrically symmetric textures given in the present section has the virtue of being exact. It is therefore worthwhile to explore the regime amenable to both methods in order to verify the validity of the adiabatic approximation scheme. It is natural to anticipate that the adiabatic approximation is accurate for large magnetic fields in order to satisfy the criterion, discussed at the beginning of Sec. IV D, that the precession frequency ω_B should far exceed the orbital frequency ω_O. With this in mind we shall examine the *exact* solution in the limit

$$\Delta|l\sin\chi|\ll g\mu B \tag{6.17}$$

and confirm that in this limit we recover the results obtained in Sec. V.

The expansion of the spectrum is most easily accomplished by rewriting it in the following way:

$$E_{l,\alpha}(\xi,\zeta) = \Delta[(l-\phi^{\rm em})^2 + (1+2\xi)^2/4] - \alpha b\Delta\sqrt{1+2\zeta\cos\chi+\zeta^2} \tag{6.18}$$

$$\times\left[[1+b^{-1}(l-\phi^{\rm em})(1+2\xi)\cos\chi]\sqrt{1+\left(\frac{b^{-1}(l-\phi^{\rm em})(1+2\xi)\sin\chi}{1+b^{-1}(l-\phi^{\rm em})(1+2\xi)\cos\chi}\right)^2}+O(l\zeta/b)\right], \tag{6.19}$$

where we have retained the magnetization source term only to leading order. One now recognizes the existence of a combination of variables $(l/b)\sin\chi$ which will serve as a suitable small parameter. Expanding the square root in Eq. (6.19) in powers of $(l/b)\sin\chi$ we find, after a little algebra,

$$E_{l,\alpha}(\xi,\zeta) \approx \Delta[l+1/2-\phi^{\rm em}-\alpha(1+2\xi)\phi^g-\alpha\xi]^2 + \Delta(\xi+1/2)^2\sin^2\chi - \alpha g\mu B(1+\zeta\cos\chi), \tag{6.20}$$

where ϕ^g is given in Eq. (5.20), and we have omitted terms of order $(l/b)^3$ and $(l\zeta/b)$.

Thus, to leading order and in the absence of source terms, we find that the spectrum becomes

$$E_{l,\alpha} \approx \mathcal{E}_{l+1/2,\alpha} + \tfrac{1}{4}\Delta\sin^2\chi\,, \tag{6.21}$$

i.e., precisely that identified from the adiabatic approximation, Eq. (5.3), apart from an overall χ-dependent (but quantum-number-independent) constant $(\Delta/4)\sin^2\chi$ which we shall discuss below. In addition to the spectrum $E_{l,\alpha}(0,0)$ we also need the derivatives

$$\partial_{\phi^{\rm em}}E_{l,\alpha}(0,0) \approx -2\Delta(l+1/2-\Phi_\alpha), \tag{6.22a}$$

$$\partial_\xi E_{l,\alpha}(\xi,0)\big|_{\xi=0} \approx \Delta\sin^2\chi - 2\Delta\cos\chi\;\alpha(l+1/2-\Phi_\alpha), \tag{6.22b}$$

$$\partial_\zeta E_{l,\alpha}(0,\zeta)\big|_{\zeta=0} \approx -\alpha g\mu B\cos\chi\,. \tag{6.22c}$$

Inserting the first of these derivatives into Eq. (6.8) we recover the charge current, Eq. (5.4), with the geometric phase given by Eq. (5.20). Inserting the second derivative into Eq. (6.10) we recover the spin current, Eq. (5.22). Inserting the third derivative into Eq. (6.12) we recover the magnetization, Eq. (5.23).

Thus, for $b^{-1}|l\sin\chi| \ll 1$ the exact diagonalization reproduces the currents and magnetization in the symmetric texture found in Sec. V using the path integral and adiabatic approximation. In other words $b^{-1}|l\sin\chi| \ll 1$ *defines* the adiabatic limit. It is instructive to eliminate the quantum number l from the adiabaticity criterion in the following way. Due to the Boltzmann factor, e.g., in Eq. (6.8), there is a cutoff l_c in the angular momentum quantum numbers l so that only those l for which $|l| \lesssim l_c$ contribute significantly in the calculation of observables. Bearing in mind the fact that l is *half*-integral, so that $|l|$ cannot be smaller than $\frac{1}{2}$, we see that $l_c = \max\left(\frac{1}{2}, 1/\sqrt{\beta\Delta}\right)$. Hence, the adiabaticity criterion becomes $b \gg l_c|\sin\chi|$. If $\beta\Delta < 4$, then the criterion reads $b \gg |\sin\chi|/\sqrt{\beta\Delta}$, i.e., $\beta g\mu B \gg \sqrt{\beta\Delta}|\sin\chi|$. On the other hand, if $\beta\Delta > 4$, then it reads $b \gg |\sin\chi|/2$, i.e., $2g\mu B \gg \Delta|\sin\chi|$. In particular, in the low-temperature limit the criterion for adiabaticity is independent of temperature.

We have shown that, in the case of the *symmetric* texture, the criterion for the validity of the path-integral adiabatic approximation is that $b^{-1}|l|\sqrt{1-|\mathbf{N}|^2} \ll 1$, where we have used Eq. (5.21b). It is therefore reasonable to suppose that this criterion also applies to *arbitrary* textures, with $\mathbf{N}$ given by Eq. (5.9b), provided the textures are not too rough.

F. Quantum fluctuations and zero-point energy

Until now, we have focused our attention on physical quantities for which the adiabatic approximation is reliable. Not surprisingly, there are physical quantities, primarily associated with quantum fluctuations, which are not correctly obtained using the path-integral adiabatic approach, even within the adiabatic limit. The reason for this is that, as mentioned in Sec. IV, the adiabatic approximation for the spin propagator is only accurate for slowly varying magnetic fields. However, there are certainly paths in the path integral which are rough. These rough paths cause the spin to experience a rapidly varying field and hence not to evolve adiabatically.

Let us explore this issue a little further by rewriting the integrand of the propagator in Eq. (4.15) as

$$\exp(-S_{\alpha_f,\alpha_i}[\theta]) = \exp(-S^{\rm orb}_{\alpha_f,\alpha_i}[\theta] - S^s_{\alpha_f,\alpha_i}[\theta]),$$

where (6.23)

$$S^s_{\alpha_f,\alpha_i}[\theta] = -\ln\langle\alpha_f|\hat{U}_\theta(\beta)|\alpha_i\rangle\,.$$

For the sake of simplicity we shall assume that $B(\theta)$ and $V(\theta)$ are constants. Following the usual scheme, we examine the stationary point of the action, i.e., the solution of $\delta S = 0$. Assuming the validity of the adiabatic approximation, we see that $\delta S^s = 0$ and thus does not influence the classical equation of motion for $\theta(\tau)$. If we find, as one usually does, a smooth classical path $\theta^{\rm cl}(\tau)$, then this procedure is at least self-consistent. Continuing with the usual scheme, we examine the quantum fluctuations $\eta(\tau)$ around the classical path by analyzing $S[\theta^{\rm cl}+\eta] = S^{\rm orb}[\theta^{\rm cl}+\eta] + S^s[\theta^{\rm cl}+\eta]$. Now $S^{\rm orb}$ is quadratic and therefore presents no difficulties. By contrast, we are unable to compute S^s for an arbitrary path. Whereas it was reasonable to evaluate S^s within the adiabatic approximation in solving the classical equation of motion, such an assumption may no longer be valid for calculating $S^s[\theta^{\rm cl}+\eta]$ because $\eta(\tau)$ is typically rough. In particular, this means that rather than vanishing identically, as does

$$DS^s[\theta^{\rm cl}+\eta] \equiv S^s[\theta^{\rm cl}+\eta] - S^s[\theta^{\rm cl}] \tag{6.24}$$

within the adiabatic approximation, DS^s is sensitive to

typical fluctuations η and therefore modifies the action

$$DS[\theta^{\rm cl}+\eta] \equiv S[\theta^{\rm cl}+\eta] - S[\theta^{\rm cl}] \tag{6.25}$$

controlling these fluctuations. Writing the propagator Eq. (4.15) schematically in terms of the fluctuation path integral for a given winding number ν, i.e.,

$$G_\nu \sim e^{-S[\theta^{\rm cl}]}\, e^{-DF[\theta^{\rm cl}]}, \tag{6.26a}$$

$$e^{-DF[\theta^{\rm cl}]} \sim \int \mathcal{D}\eta\; e^{-DS[\theta^{\rm cl}+\eta]}, \tag{6.26b}$$

we recognize that our path-integral calculation in Sec. IV essentially replaces DS by $DS^{\rm orb}$. However, the inclusion of DS^s generally modifies the fluctuation contribution to the partition function Z. If this modification should contain a term which is independent of ν, then such a term could be interpreted as a state-independent additive correction to the energy spectrum due to quantum fluctuations, i.e., zero-point energy. Now, the adiabatic expansion of the exact spectrum for the symmetric texture, Eq. (6.21), differs from the spectrum identified from the path-integral approach (given in Sec. IV) by the constant term $(\Delta/4)\sin^2\chi$. The origin of this discrepancy lies in the omission of DS^s from the analysis of the quantum fluctuations.

For the calculation of quantities such as the persistent currents and magnetization, this additive constant in the spectrum cancels and is therefore irrelevant. However, for other quantities, such as the mean-square z component of the total angular momentum $\hat{L}^3 = p_\theta + (\hbar/2)\hat{\sigma}^3$, this cancellation does not occur. To see this, we consider the planar symmetric texture $\chi = \pi/2$, with $\phi^{\rm em} = 0$, for which the exact diagonalization gives $\langle \hat{L}^3 \rangle = 0$ (see the beginning of Sec. VI D). Next, we consider the square of the total angular momentum, and compute its expectation value at zero temperature, obtaining

$$\langle (\hat{L}^3)^2 \rangle_0 = \tfrac{1}{4}\hbar^2 + \hbar^2 \langle \hat{J}^3 \rangle_0 + \langle (\hat{p}_\theta)^2 \rangle_0 , \tag{6.27}$$

where $\langle \hat{J}^3 \rangle_0$ is given in Eq. (6.16) and

$$\langle (\hat{p}_\theta)^2 \rangle_0 = -\lim_{T\to 0} \frac{\hbar^2}{\beta}\frac{\partial}{\partial\Delta} \ln Z = \frac{\hbar^2}{2}\left(1 - \frac{1}{\sqrt{1+4b^2}}\right). \tag{6.28}$$

Thus, we find the exact result $\langle (\hat{L}^3)^2 \rangle_0 = \hbar^2/4$, a result which of course also holds in the adiabatic approximation (i.e., $b \gg 1$) of the exact spectrum, Eq. (6.21). However, in the path-integral adiabatic approximation we obtain, using Eqs. (5.22) and (5.2c), $\langle (\hat{p}_\theta)^2 \rangle_0 \approx \hbar^2/4$ and thus $\langle (\hat{L}^3)^2 \rangle_0 \approx 0$. This example involving mean-square quantities shows explicitly that the path-integral adiabatic approximation can be unreliable for quantities which are sensitive to quantum fluctuations or zero-point energy.

VII. EQUILIBRIUM CURRENTS FOR MANY FERMIONS

We shall now consider persistent currents and magnetization in a many-particle system of spin-$\frac{1}{2}$ fermions, continuing to neglect particle-particle interactions. Within the grand canonical ensemble and at nonzero temperatures this would amount to replacing the Boltzmann weight $Z^{-1}\exp(-\beta\epsilon_i)$ by the Fermi-Dirac distribution $f(\epsilon_i) = [\exp\beta(\epsilon_i - \mu) + 1]^{-1}$, where μ is the chemical potential and ϵ_i is the single-particle energy spectrum. In particular, for the symmetric texture the exact solution has a spectrum given by Eq. (6.6). For arbitrary textures the exact spectrum is not available, but in the adiabatic approximation it is given by Eq. (5.3). We shall focus here on the results for the many-particle currents and magnetization in the adiabatic approximation. In addition, we shall restrict our attention to fixed particle number M, which corresponds to the typical experimental arrangement, and to $T = 0$. This amounts to populating a Fermi sea up to the Fermi energy ϵ_F. The many-particle ground state energy is then given by $E = \sum_{n,\alpha} \mathcal{E}_{n,\alpha}$, where the summation includes the M lowest-lying single-particle energy levels, consistent with the Pauli principle. According to Eqs. (5.4), (5.10), and (5.16) the (dimensionful) many-particle charge current j^0, spin current $\mathbf{j}$, and magnetization $\mathbf{s}$ can be expressed in terms of E by

$$j^0 \approx -\frac{q\hbar}{2\pi m a^2}\frac{1}{2\Delta}\frac{\partial E}{\partial \phi^{\rm em}}, \tag{7.1a}$$

$$\mathbf{j} \approx \frac{\hbar^2}{4\pi m a^2}\left(M\,\mathbf{F} - \frac{1}{2\Delta}\frac{\partial E}{\partial \phi^g}\mathbf{N}\right), \tag{7.1b}$$

$$\mathbf{s} \approx -\frac{\hbar}{2}\frac{1}{g\mu}\frac{\partial E}{\partial B}\mathbf{N}. \tag{7.1c}$$

To address the applicability of the adiabatic approximation in Fermi systems we introduce the Fermi orbital angular momentum number $n_F \equiv \sqrt{\epsilon_F/\Delta}$. Then criterion (6.17) shows that the adiabatic approximation can be applied to all occupied states of the Fermi sea provided that $n_F \ll b$, i.e., $hv_F/2L \ll g\mu B$, where v_F is the Fermi velocity and $L = 2\pi a$ is the circumference of the ring. Equivalently, this requires that the orbital level splitting at the Fermi surface $\delta\epsilon_F \sim 2\sqrt{\epsilon_F\,\Delta}$ be much less than the Zeeman level splitting $2g\mu B$.

For the sake of illustration, consider a system with the following parameters, consistent with the experimental configuration of Chandrasekhar *et al.*:[6] a single Au loop of circumference $L \approx 7.5\,\mu$m, Fermi velocity $v_F \approx 1.4 \times 10^6\,{\rm ms}^{-1}$, and $g \approx 2$. Then the criterion for adiabaticity to be maintained throughout the Fermi sea is that the applied magnetic field exceed approximately 6.6 T. If the Au loop were replaced by one made of GaAs, then the Fermi velocity would be reduced to approximately $3 \times 10^5\,{\rm ms}^{-1}$; correspondingly the magnetic field required to maintain adiabaticity would be reduced to approximately 1.4 T.

Following the arguments described in Ref. 4, and applying them to Eqs. (7.1a), (7.1b), and (7.1c), we find that the order of magnitude of the charge current for a typical texture is given by $j^0_{\rm max} \sim qv_F/L$ and, similarly, for the spin current $|\mathbf{j}|_{\rm max} \sim \hbar v_F/2L$. As a consequence, for the experimental system of the single Au loop described in the preceding paragraph one may, e.g.,

anticipate an electric field caused by the persistent spin current, with magnitude $2 \times 10^{-7}\,\mathrm{Vm}^{-1}$ at a location roughly $2\,\mu$m along the loop axis from the loop center. The detailed development of these estimates is somewhat involved and is planned to be described in a forthcoming paper.[9] In Ref. 9 we shall also estimate the magnitudes of the static magnetic and electric fields produced, respectively, by the persistent charge current and spin current and, in particular, their dependence on the texture and the electromagnetic flux.

VIII. SUMMARY AND OUTLOOK

In this paper we have considered an idealized model of a mesoscopic ring containing noninteracting spin-$\frac{1}{2}$ particles coupled to a static inhomogeneous magnetic field via a Zeeman term. We have constructed a path integral for the thermal propagator, in which spin and orbital motion are decoupled, in the presence of an arbitrary texture. Within an adiabatic approximation for the (imaginary-time) spin dynamics, and for textures with constant magnitude but arbitrary local orientation, we have computed the persistent charge current, spin current, and magnetization. We have identified a geometrical aspect of the texture — the geometric vector — which, in addition to the well-known Berry phase, characterizes the spin current. We have discussed an exact diagonalization for the case of symmetric textures, and have analyzed the limit in which this approach and path-integral calculation are equivalent. In addition, we have discussed the roles of quantum fluctuations and zero-point energy. Finally, we have given results for persistent currents and magnetization for a system of many noninteracting spin-$\frac{1}{2}$ fermions.

The results developed in this paper can be applied to a range of physical systems including systems of charged particles, such as normal metals and semiconductors, and neutral particles, such as normal ^{3}He and ^{3}He-^{4}He mixtures. Detailed numerical estimates of the magnitudes of the magnetic and electric fields produced by persistent currents is planned to be presented, *inter alia*, in a forthcoming paper.[9] Applications to elastic, optical, and superfluid systems may also be anticipated. Furthermore, the techniques developed here are also applicable to nonequilibrium phenomena such as the recently predicted Berry-phase-induced magnetoconductance oscillations in multiply connected structures,[34] and other *real-time* interference phenomena. Finally, in the spirit of Hannay's classical analog of the Berry phase,[35] it would be interesting to find a classical analog of the geometric vector.

ACKNOWLEDGMENTS

It is a pleasure to thank Alexander Balatsky, Jeffrey Cina, Eduardo Fradkin, Jack Mochel, Kieran Mullen, Michael Stone, and, in particular, Tony Leggett for helpful conversations, and Stephen Wolfram for providing us with a copy of MATHEMATICA.™ D.L. gratefully acknowledges support from the Swiss National Science Foundation and the John D. and Catherine T. MacArthur Foundation at the University of Illinois. P.M.G. gratefully acknowledges support from the U.S. National Science Foundation through Grants DMR-91-22385 and through DMR-91-57018.

---

*Present address: IBM Thomas J. Watson Research Center, Yorktown Heights, New York 10598.

†E-mail address: p-goldbart@uiuc.edu. Also at Materials Research Laboratory, University of Illinois at Urbana-Champaign, 104 South Goodwin Avenue, Urbana, Illinois 61801; Beckman Institute for Advanced Science and Technology, 405 Mathews Avenue, Urbana, Illinois 61801.

[1] Y. Aharonov and D. Bohm, Phys. Rev. **115**, 485 (1959).

[2] For a review, see S. Washburn and R. A. Webb, Adv. Phys. **35**, 375 (1986).

[3] M. Büttiker, Y. Imry, and R. Landauer, Phys. Lett. **96A**, 365 (1983); R. Landauer and M. Büttiker, Phys. Rev. Lett. **54**, 2049 (1985); H. F. Cheung, Y. Gefen, E. K. Riedel, and W.-H. Shih, Phys. Rev. B **37**, 6050 (1988); N. Trivedi and D. A. Browne, *ibid.* **38**, 9581 (1988); H. Bouchiat and G. Montambaux, J. Phys. (Paris) **50**, 2695 (1989); G. Montambaux, H. Bouchiat, D. Sigeti, and R. Friesner, Phys. Rev. B **42**, 7647 (1990); V. Ambegaokar and U. Eckern, Phys. Rev. Lett. **65**, 381 (1990); Y. Fu and C. Park (unpublished); A. Schmid, Phys. Rev. Lett. **66**, 80 (1991); F. von Oppen and E. K. Riedel, *ibid.* **66**, 84 (1991); U. Eckern (unpublished); B. L. Altshuler, Y. Gefen, and Y. Imry, Phys. Rev. Lett. **66**, 88 (1991).

[4] D. Loss and P. Goldbart, Phys. Rev. B **43**, 13 762 (1991).

[5] L. P. Lévy, G. Dolan, J. Dunsmuir, and H. Bouchiat, Phys. Rev. Lett. **64**, 2074 (1990).

[6] V. Chandrasekhar, R. A. Webb, M. J. Brady, M. B. Ketchen, W. J. Gallagher, and A. Kleinsasser, Phys. Rev. Lett. **67**, 3578 (1991).

[7] M. V. Berry, Proc. R. Soc. London, Ser. A **392**, 45 (1984).

[8] For a collection of relevant reprinted articles and commentary, see A. Shapere and F. Wilczek, *Geometric Phases in Physics* (World Scientific, Singapore, 1989).

[9] D. Loss and P. Goldbart (unpublished).

[10] D. Loss, P. Goldbart, and A. V. Balatsky, Phys. Rev. Lett. **65**, 1655 (1990).

[11] A. Messiah, *Quantum Mechanics Vol. II* (Wiley, New York, 1962), Chap. XVII.

[12] A tight-binding model with spin-dependent hopping, which can also lead to a geometric phase, has been studied by Y. Meir, Y. Gefen, and O. Entin-Wohlman, Phys. Rev. Lett. **63**, 798 (1989).

[13] Quite generally, the spin current is, of course, a second rank tensor $(\hat{p}_j - q\hat{A}_j)\hat{\sigma}^k$. However, the strictly one-dimensional nature of the ring allows us to restrict our attention to only the θ component of the orbital momentum and, hence, to the *vector* of spin currents $(a^{-1}\hat{p}_\theta - q\hat{A}_\theta)\,\hat{\sigma}^k$.

[14] In addition to the sample size, three further physical length scales play significant roles in mesoscopic physics: the elastic-scattering length ℓ_{el} (due to elastic collisions with static impurities), the dephasing length ℓ_φ (usually determined by inelastic processes such as electron-electron or electron-phonon scattering), and the localization length ℓ_{loc}.

[15] For a related approach to dynamical propagators, see H. Kuratsuji and S. Iida, Prog. Theor. Phys. **74**, 439 (1985).
[16] See, e.g., L. S. Schulman, *Techniques and Applications of Path Integration* (Wiley, New York, 1981).
[17] See also R. P. Feynman and A. R. Hibbs, *Quantum Mechanics and Path Integrals* (McGraw-Hill, New York, 1965).
[18] See, e.g., H. Kleinert, *Path Integrals in Quantum Mechanics Statistics and Polymer Physics* (World Scientific, Singapore, 1990), especially Chap. 6.
[19] M. Born and V. F. Fock, Z. Phys. **51**, 165 (1928).
[20] Throughout this paper we have, for the sake of convenience, suppressed the dependence of the magnetic field on the coordinates transverse to the ring. That the magnetic field does not violate the Maxwell equation $\nabla \cdot \mathbf{B} = 0$ can be ensured by allowing $\mathbf{B}$ to vary suitably in the directions transverse to the ring. Similarly, one can ensure that $\nabla \wedge \mathbf{B} = \mathbf{0}$ so that *on the ring itself* there are neither external currents nor time-varying external electric fields.
[21] Transforming to a new basis may move the location of the Dirac string on which the geometric gauge potential (introduced below) is singular; for a discussion of related issues see, e.g., Ref. 8.
[22] In fact, all we shall make use of are the matrix elements of the density matrix, i.e., the *normalized* thermal propagator, which is always bounded.
[23] M. V. Berry, Proc. R. Soc. London, Ser. A **414**, 31 (1987).
[24] For a general discussion of the Berry phase for nonclosed paths, see J. Samuel and R. Bhandari, Phys. Rev. Lett. **60**, 2339 (1988).
[25] See, for example, Milton Abramowitz and Irene Stegun, *Handbook of Mathematical Functions* (Dover, New York, 1970).
[26] Similar structure has been found, for example, by G. E. Volovik, J. Phys. C **20**, L83 (1987), M. Stone, Phys. Rev. D **33**, 1191 (1986), and by J. Moody, A. Shapere, and F. Wilczek, Phys. Rev. Lett. **56**, 893 (1986); see also Ref. 8.
[27] See, e.g., Ref. 25, Sec. 16.29.23.
[28] There is, as we have noted, a close analogy between geometric and electromagnetic fluxes. However, this analogy does not extend precisely to the final form of the currents which they cause. In particular, whereas the charge current can be expressed solely as a derivative with respect to ϕ^{em}, the same is not true for the spin current and ϕ^{g}.
[29] In fact one has a choice of surfaces Σ on the unit sphere which are bounded by a given curve $\mathcal{C}$. However, the value of $\mathbf{F}$ is insensitive to this choice, provided one pays due attention to the orientation of the surface normal, and recognizes that when Σ covers the unit sphere an integral number of times then $\int_{\Sigma} d\mathbf{S} = 0$.
[30] This can also be seen from the line integral representation of the geometric vector $\mathbf{F}$, Eq. (5.12). Decomposing $\mathbf{n}$ into components parallel and perpendicular to $\mathbf{e}^k$, i.e., $\mathbf{n} = \mathbf{n}_{\perp} + \mathbf{n}_{\parallel}$, we obtain $-4\pi F^k = \mathbf{e}^k \int_C \mathbf{n}_{\perp} \wedge d\mathbf{n}_{\perp}$. The interpretation follows from the recognition that $|\mathbf{n}_{\perp} \wedge d\mathbf{n}_{\perp}|$ is twice the element of area in the plane perpendicular to $\mathbf{e}^k$. Alternatively, one may regard $\mathbf{F}$ as the flux through Σ of the tensor field $\sum_k \mathbf{e}^k \otimes \mathbf{e}^k$.
[31] See, e.g., J. D. Jackson, *Classical Electromagnetism* (Wiley, New York, 1975).
[32] We mention that the low-temperature limit of the charge current given in Ref. 10 applies only to the interval $0 \leq \chi < \pi/2$, where χ is the tilt angle of Eq. (5.19).
[33] See, e.g., G. Herzberg and H. C. Longuet-Higgins, Disc. Faraday Soc. **35**, 77 (1962); V. Romero-Rochin and J. A. Cina, J. Chem. Phys. **91**, 6103 (1989).
[34] D. Loss, P. Goldbart, and A. V. Balatsky, in *Granular Nanolelectronics, Proceedings of the NATO Advanced Study Institute, Il Ciocco, Italy, 1990*, edited by D. K. Ferry, J. R. Barker, and C. Jacoboni, *NATO Advanced Study Institute Series B: Physics* (Plenum, New York, 1991), Vol. 251, p. 539; see also A. Stern [Phys. Rev. Lett. **68**, 1022 (1992)].
[35] J. H. Hannay, J. Phys. A **18**, 221 (1985); see also Ref. 8.

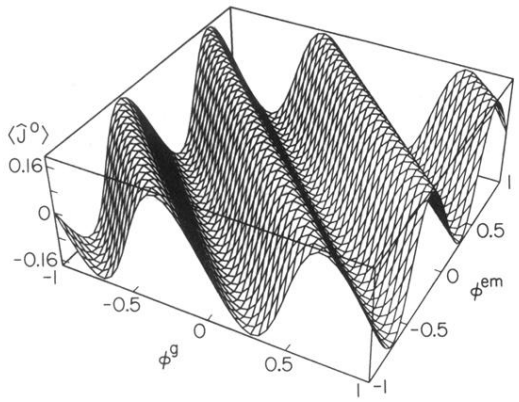

FIG. 2. The (dimensionless) charge current $\langle \hat{J}^0 \rangle$ as a function of the electromagnetic flux ϕ^{em} and the geometric flux ϕ^g at temperature $T = 1$ mK for a ring of radius $a = 3000$ Å and for a magnetic field of magnitude $B = 50$ G.

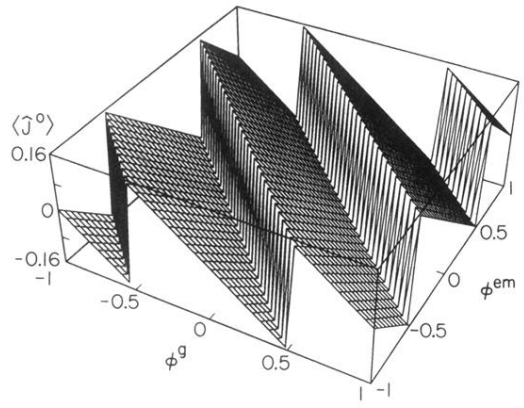

FIG. 3. The zero-temperature (dimensionless) charge current $\langle \hat{J}^0 \rangle_0$ as a function of the electromagnetic flux ϕ^{em} and the geometric flux ϕ^g.

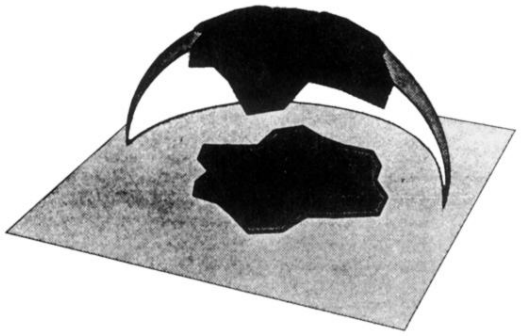

FIG. 4. Geometrical interpretation of the flux ϕ^g and the vector $\mathbf{F}$. The geometric flux corresponds to the area of the shaded part of the spherical surface Σ. The component F^3 of the geometric vector corresponds to the area of the shaded part of the equatorial plane, i.e., to the area of the projection of Σ on to the equatorial plane.

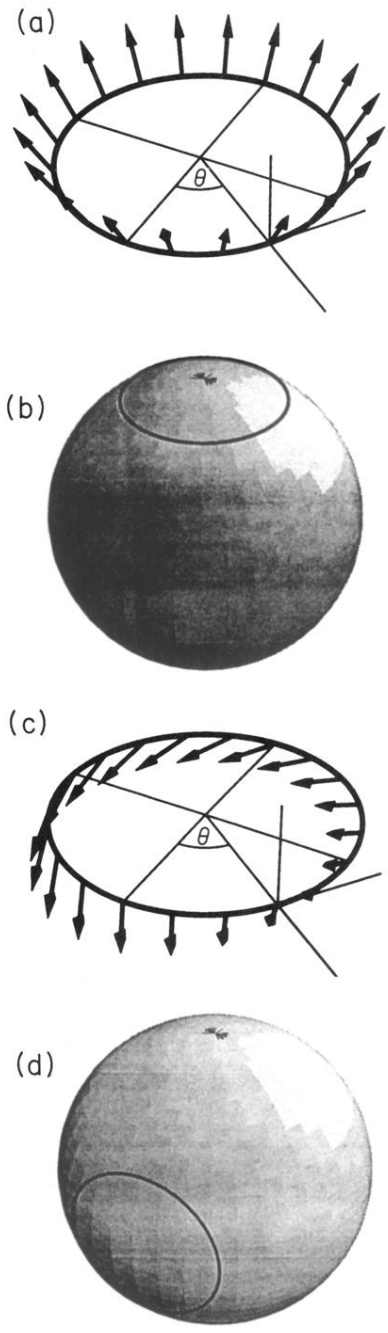

FIG. 5. Two textures related by a global rotation, each represented in two ways: (i) as the magnetic field around a ring [(a) and (c)], and (ii) as trajectories on the unit sphere [(b) and (d)].